

**DEVELOPMENT AND CHARACTERISATION OF METFORMIN LOADED FILM  
WITH FLAXSEED GEL FOR ACCELERATION OF HEALING PROCESS OF BURN  
WOUNDS: AN APPROACH FOR TISSUE REGENERATION**

Thesis submitted in partial fulfilment for the requirement of the  
**Degree of Master of Pharmacy**

by

**Pratyusa Sar**

M.Pharm, 2<sup>nd</sup> Year 2<sup>nd</sup> Sem.

Class Roll No: 002011402027

Examination Roll No. :M4PHB22002

Registration No:154288 of 2020-2021

Under the Guidance of

**Prof. (Dr.) Amalesh Samanta**

Division of Microbiology & Pharmaceutical Biotechnology

**DEPARTMENT OF PHARMACEUTICAL TECHNOLOGY**

**Faculty Council of Engineering & Technology**

**Jadavpur University**

Kolkata- 700032

2022

**CERTIFICATE OF APPROVAL**

This is to certify that the thesis entitled "**DEVELOPMENT AND CHARACTERISATION OF METFORMIN LOADED FILM WITH FLAXSEED GEL FOR ACCELERATION OF HEALING PROCESS OF BURN WOUNDS: AN APPROACH FOR TISSUE REGENERATION**" submitted to Jadavpur University, Kolkata for the partial fulfilment of the Master Degree in Pharmacy, is a faithful record of bonafide and original research work carried out by Ms. Pratyusa Sar bearing Class Roll No. 002011402027 and Registration No. 154288 of 2020-2021 under my supervision and guidance.

*[Signature]*  
24/8/22

Head  
Dept. of Pharmaceutical Technology  
Jadavpur University  
Kolkata - 700 032, W.B. India

Prof. (Dr.) Sanmay Karmakar  
Head of the Department  
Department of Pharmaceutical Technology  
Jadavpur University,  
Kolkata- 700032

*[Signature]*  
24-8-22

Prof. (Dr.) Amalesh Samanta  
Division of Microbiology & Pharmaceutical  
Biotechnology  
Department of Pharmaceutical Technology,  
Jadavpur University,  
Kolkata- 700032

*Prof. (Dr.) Amalesh Samanta*  
*Div. of Microbiology & Biotechnology*  
*Dept. of Pharmaceutical Technology*  
*Jadavpur University*  
*Kolkata-700032, India*

*[Signature]*  
24/8/22

Dean  
Faculty Council of Engineering and Technology,  
Jadavpur University,  
Kolkata-700032



**DEAN**  
Faculty of Engineering & Technology  
JADAVPUR UNIVERSITY  
KOLKATA-700 032

### **Declaration of the Originality and Compliance of Academic Ethics**

I, Pratyusa Sar, a student of M.Pharm, 2<sup>nd</sup> year, bearing Roll No: 002011402027, Registration No. 154288 of 2020-2021 studying in Department of Pharmaceutical Technology, Jadavpur University, Kolkata-32, hereby declare that my thesis work titled – “**DEVELOPMENT AND CHARACTERISATION OF METFORMIN LOADED FILM WITH FLAXSEED GEL FOR ACCELERATION OF HEALING PROCESS OF BURN WOUNDS: AN APPROACH FOR TISSUE REGENERATION**”, is original and presented in accordance with academic rules and ethical conduct and no part of this project work has been submitted for any other degree of mine. All the information and works are true to the best of my sense and knowledge.

**Name:** Pratyusa Sar

**Class Roll No.:** 002011402027

**Registration No.:** 154288 of 2020-2021

**Signature with date:** Pratyusa Sar  
24.8.2022

**Place:** Jadavpur, Kolkata.

## ACKNOWLEDGEMENT

I believe it to be a privilege to work under the guidance of Prof. (Dr.) Amalesh Samanta, Division of Microbiology & Pharmaceutical Biotechnology, Jadavpur University on the innovative topic “DEVELOPMENT AND CHARACTERISATION OF METFORMIN LOADED FILM WITH FLAXSEED GEL FOR ACCELERATION OF HEALING PROCESS OF BURN WOUNDS: AN APPROACH FOR TISSUE REGENERATION.” I am fortunate to have his supportive and helpful direction throughout my work period. I was able to accomplish this job without difficulty because of his expert advice and enormous compassion at every level of my work.

I also express my sincere gratitude to our H.O.D., Department of Pharmaceutical Technology, Jadavpur University, Prof. (Dr.) Sanmay Karmakar for providing me an opportunity to do my thesis work successfully.

I am grateful to All India Council for Technical Education (AICTE), Government of India for providing financial support .

I express my heartfelt gratitude to Ph.D. scholars –Piu Das, Ahana Hazra, Mousumi Tudu, Anurag Banerjee, Anirban Ghosh, Sohini Chatterjee, Abhishek Mohanta; PG students: Totan Roy, Pankaj Paul; UG students Dhiman Mahata, Md. Hakim.

With great sorrow, I express my deep feelings for innocent rats, who sacrificed their lives for betterment of mankind. I hope their sacrifice will add more ray of hope in saving lives of people. Please God may their souls rest in peace.

Special thanks to C I Laboratories for providing Metformin as gift sample.

Special thanks to our laboratory maintenance staff Mr. Deepak Balmiki for keeping our workspace clean and hygienic.

I will always be indebted to The Almighty, my parents and my family members, whose unwavering commitment to me has led to this point in my life.

I would also want to express my gratitude to my friends and everyone else for their cooperation and assistance during the course of the project.

-----  
**Pratyusa Sar**

## INDEX

<b>Sl. NO.</b>	<b>CONTENTS</b>	<b>PAGE NO.</b>
	List of figures	
	List of tables and charts	
	List of abbreviations	
	Abstract	
	Chapter 1	
<b>1</b>	Introduction	<b>1-12</b>
<b>1.1</b>	Pathophysiology of burn wound	<b>2</b>
<b>1.2</b>	Stages of wound healing	<b>3-4</b>
<b>1.3</b>	Complexities of wound healing	<b>4</b>
<b>1.4</b>	Factors affecting wound healing	<b>5-6</b>
<b>1.5</b>	Burn wound and its types	<b>6-7</b>
<b>1.6</b>	Anatomy and physiology of normal skin	<b>7-8</b>
<b>1.7</b>	Classification of burn wounds	<b>8</b>
<b>1.8</b>	Burn wound model	<b>9</b>
<b>1.9</b>	Normal mechanism of burn wound healing	<b>10</b>
<b>1.10</b>	Mechanism of action of Metformin in healing process of burn wound	<b>11-12</b>
	Chapter 2	
<b>2</b>	Literature review	<b>13-15</b>
	Chapter 3	
<b>3</b>	Aim and objective	<b>16</b>
	Chapter 4	
<b>4.1</b>	Experimental	<b>18-28</b>
<b>4.1.1</b>	Reagents and materials	<b>18-20</b>
<b>4.2</b>	Methodology	<b>21</b>

<b>4.2.1</b>	Preparation of flaxseed extract	<b>21</b>
<b>4.2.2</b>	Preparation of the formulation	<b>21</b>
<b>4.3</b>	Optimisation	<b>22</b>
<b>4.3.1</b>	Physical characteristics	<b>22</b>
<b>4.3.2</b>	Moisture content study	<b>22</b>
<b>4.3.3</b>	Water solubility	<b>22</b>
<b>4.3.4</b>	Transparency test	<b>23</b>
<b>4.3.5</b>	Water Vapour Permeability Test	<b>23</b>
<b>4.3.6</b>	Swelling Index	<b>23</b>
<b>4.3.7</b>	Dehydration rate	<b>24</b>
<b>4.3.8</b>	Rate of absorption	<b>24</b>
<b>4.3.9</b>	<i>In-vitro</i> drug release studies	<b>24-25</b>
<b>4.3.10</b>	Drug Entrapment Efficiency	<b>25</b>
<b>4.3.11</b>	FT-IR analysis	<b>25</b>
<b>4.3.12</b>	SEM studies	<b>26</b>
<b>4.3.13</b>	XRD analysis	<b>26</b>
<b>4.3.14</b>	TGA-DSC analysis	<b>26</b>
<b>4.4</b>	<i>In-vivo</i> studies	<b>27-28</b>
<b>4.4.1</b>	Animals and Ethics Statement	<b>27</b>
<b>4.4.2</b>	Creation of burn wound model	<b>27</b>
<b>4.2.3</b>	Experimental design	<b>28</b>
	Chapter 5	
<b>5.1</b>	Results	<b>29-41</b>
	Chapter 6	
<b>6.1</b>	Discussion	<b>42-47</b>
	Chapter 7	
<b>7.1</b>	Conclusion	<b>48</b>
	Chapter 8	
<b>8.1</b>	References	<b>49-61</b>

**LIST OF FIGURES:**

FIG 1	STAGES OF WOUND HEALING
FIG 2	COMPLEXITIES OF WOUND HEALING
FIG 3	DEGREES OF BURN WOUND ALONG WITH STRUCTURE OF SKIN
FIG 4	ZONE OF BURN WOUNDS
FIG 5	DIAGRAM OF STUDY PROTOCOL
FIG 6	IMAGE OF THE METFORMIN LOADED FILM
FIG 7	IN VITRO DRUG RELEASE OF FORMULATIONS CONTAINING DIFFERENT RATIO (F1, F2, F3)
FIG 8	a.ZERO ORDER RELEASE MODEL b. FIRST ORDER RELEASE MODEL c. HIGUCHI RELEASE MODEL d. KORSEMEYER-PEPPA'S RELEASE MODEL
FIG 9	FT-IR ANALYSIS OF FORMULATION, CARBOPOL, PECTIN, METFORMIN
FIG 10	SEM IMAGES OF BLANK FILM AND DRUG LOADED FILM
FIG 11	XRD IMAGES a. METFORMIN b. FORMULATION
FIG 12	DSC THERMOGRAM OF a. METFORMIN b. FORMULATION
FIG 13	IMAGE OF CONTROL GROUP'S PSEUDOESCHAR
FIG 14	IMAGES OF ANIMAL MODELS ON ALTERNATIVE DAYS SHOWING THE WOUND CONTRACTION RATE

**LIST OF TABLES AND CHARTS:**

TABLE 1	TYPES OF BURN INJURY
TABLE 2	CLASSIFICATION OF BURN WOUNDS
TABLE 3	ENTRAPMENT EFFICIENCY AND SWELLING BEHAVIOUR OF FILMS
TABLE 4	EXPERIMENTAL GROUP OF ANIMALS
CHART 1	WOUND CONTRACTION RATE

**LIST OF ABBREVIATIONS:**

COX2	Cyclooxygenase-2
DALYs	Disability-Adjusted life-years
DSC	Differential Scanning Calorimetry
ECM	Extra Cellular Matrix
ECs	Endothelial cells
Endo migr	Endodermal Migration
Endo Prolif	Endodermal Proliferation
Epi migr	Epidermal Migration
Epi Prolif	Epidermal Proliferation
FT-IR	Fourier Transform Infrared Spectroscopy
GLUT4	Glucose transporter type 4
GT	Granulation Tissue
HIF-1	Hypoxia-Inducible Factor-1
HPA Axis	Hypothalamic Pituitary Adrenal Axis
iNOS	inducible Nitric Oxide Synthase
JNK	c-Jun N-terminal kinase
MMP	Matrix Metallo Proteinase
mTOR	Mammalian Target of Rapamycin
NLRP3	NOD Like Receptor P3
PDGF	Platelet-Derived growth factor
PKC	Protein Kinase C
PTEN	Phosphatase and TENsin homolog deleted on chromosome 10
ROS	Reactive Oxygen Species
SEM	Scanning Electron Microscope
TGF- $\beta$	Transforming Growth Factor- $\beta$
TIMP	Tissue Inhibitors of Metalloproteinases
VEGF	Vascular Endothelial Growth Factor
WVTR	Water Vapor Transmission Rate
XRD	X-Ray Diffraction



## **ABSTRACT:**

Burn injuries are one of the leading problems of death all over the world. It is different from other wounds as the chances of contamination and secondary infection in case of burn wound progresses with time whereas other kind of wounds get contaminated and infected from the very first moment but heals with time. For this reason, burn injuries are difficult to treat and chances of morbidity are high from those kind of burn wounds which do not seem to be dangerous. The thing which makes burn injury more traumatic is the dressing process, which causes enormous pain to the patient and sometimes it comes with bleeding. Moreover, the marketed drugs stain the place of wound and causes hindrance in healing procedure too as it leaves the area dry. If burn injuries are treated with moist approach, the chances of scar formation get less, and the wound heals faster. For this reason, the goal of the project was to form such a biodegradable adhesive film which will be easy to apply and advantageous for dressing purpose also. Metformin, a biguanide drug, used for treating diabetic patients has been used in this formulation as it shows wound healing potential by blocking NLRP3 inflammasome and boosting the polarization of M2 macrophage. Both *in-vitro* and *in-vivo* studies are performed. For choosing the correct ratio of polymers WVTR, swelling index and other tests were done. FT-IR, SEM, XRD and DSC studies of the optimized film were performed to check the compatibility of the polymers. This study reveals effect of metformin in acceleration of healing process of burn injuries when applied topically.

Keywords: Metformin, film, 2<sup>nd</sup> degree burn wound, flaxseed, NLRP3 inflammasome, M2 Macrophage polarization

# INTRODUCTION

## **1.INTRODUCTION:**

Skin is the most significant barrier to the body (1). An open wound is a form of injury in which the skin is ripped, slashed, or perforated, causing normal anatomic structure and function to be disrupted. Normal wound healing comprises a well-coordinated process of cell migration, proliferation, and extracellular matrix deposition that goes through three separate but overlapping phases of inflammation, proliferation, and maturation leading to tissue remodeling (2). In some diseases like- diabetic ulcers, pressure ulcers, dental lacerations, and disabling conditions like an accident, the normal wound healing process is disrupted and takes more time to heal. Burn injury is an essential and challenging condition in critical care, which is now the fourth most common cause of injury (3). Priorities for specialized institutions include infection control, patient stabilization, and functional recovery optimization (4). Treatment costs for the wound can be enormous also, including the painful suffering. Especially while the dressings are used to treat burn wounds, the whole process gets quite traumatic to patients as they undergo an immense painful process. Moreover, the healing process is related directly to some factors like the patient's age and other co-morbid conditions of body.

Following are some statements regarding burn injuries all over the world according to the information from World Health Organization (WHO). Burn is an all-inclusive public health issue, with an estimated 1.8 lakhs fatalities per year, among which maximum cases occur in low and middle-income countries and almost two-thirds occur in the WHO African and South-East Asia regions. In many high-income countries, burn death rates have been decreasing, and the rate of child deaths from burns is currently over seven times higher in low- and middle-income countries than in high-income countries. Non-fatal burns are a primary source of morbidity, with consequences such as extended hospitalization, deformity, and disability, as well as stigma and rejection.

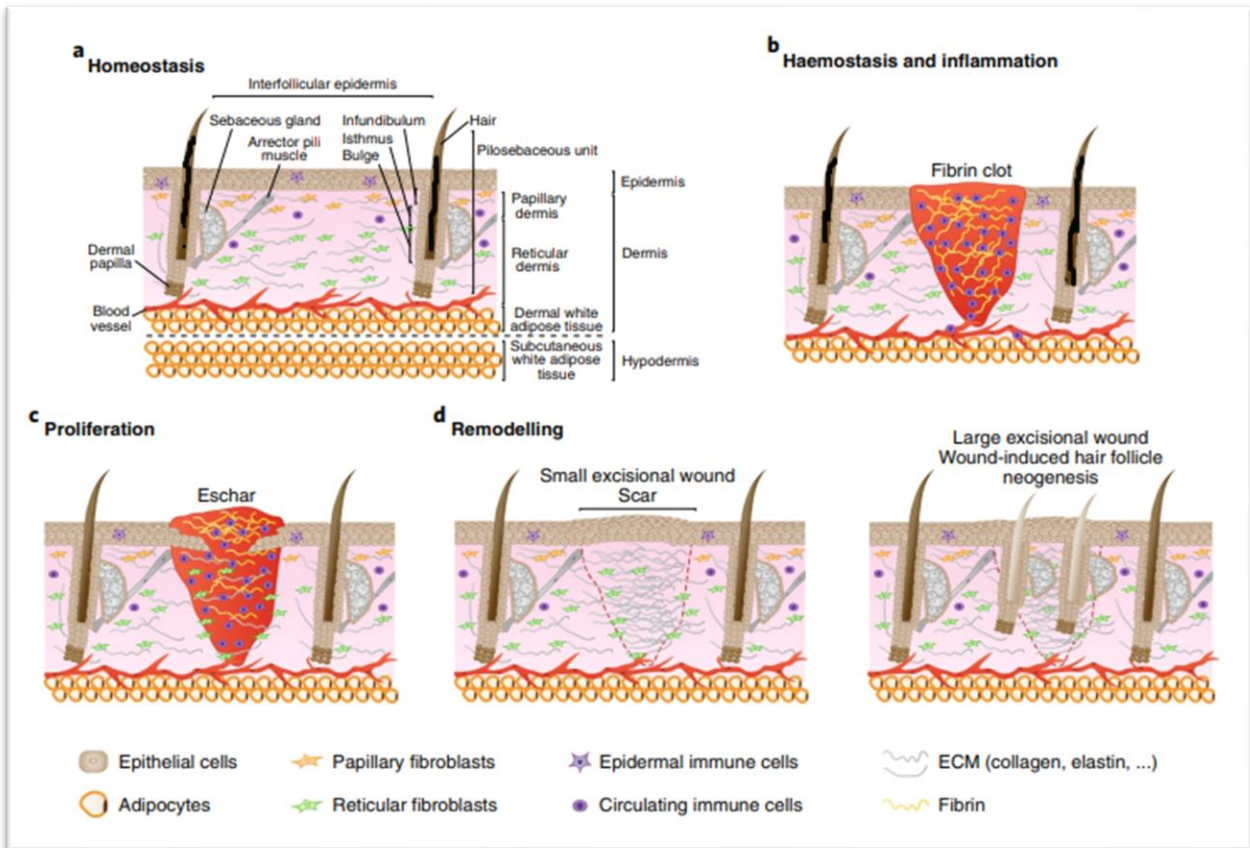
- Burns are among the top reasons of disability-adjusted life-years (DALYs) lost in low and middle-income countries (5).
- In 2004, nearly 11 million people worldwide were burned severely enough to require medical attention (5).

- Over 1,000,000 Indian people get moderately or severely burnt every year, while the number for Bangladeshi children is nearly 173,000 (5).
- In Bangladesh, Colombia, Egypt, and Pakistan, 17% of children with burns have a temporary disability, and 18% have a permanent disability (5).
- Burns is the second most common injury in rural Nepal, accounting for 5% of disabilities (5).
- In 2008, over 410,000 burn injuries occurred in the United States of America, with approximately 40,000 requiring hospitalizations (5).

### **1.1 PATHOPHYSIOLOGY OF BURN WOUND:**

The pathophysiology of the burn wound is characterized by an inflammatory response that creates edema instantly because of increased microvascular permeability, vasodilation, and extravascular osmotic activity (6). This occurs due to the direct impact of heat on the microvasculature and inflammatory chemical mediators. Histamine is released, which causes things like blood vessels and veins to dilate. Oxygen free radicals released by the Polymorphonuclear leucocytes cause damage to the cell membrane partly, which starts activating the enzymes, catalyzing the hydrolysis of prostaglandin precursor (arachidonic acid) with the quick formation of prostaglandin. As prostaglandins stop norepinephrine from being released, they may be crucial for controlling the adrenergic nerve system, which is triggered in response to heat damage (6). Following heat damage, there appears to be an increase in the number of vacuoles and a large number of open endothelial intercellular connections, according to morphological interpretations of the alterations in the functional ultrastructure of the blood lymph barrier. In addition, alterations in the interstitial tissue following burn injuries are crucial. Continuous fluid loss from blood circulation within thermally injured tissue results in elevated hematocrit levels, a fast drop in plasma volume, reduced cardiac output, and cellular hypoperfusion. Burn shock occurs if the fluids are not adequately replenished. Additionally, the burn site offers a large surface infection entry point with a significant risk of septic shock. In the current therapy of patients with severe thermal damage, four key concepts are of the highest significance: early wound closure, avoidance of septic complications, appropriate feeding, and control of the external environment (6).

## 1.2 STAGES OF WOUND HEALING :

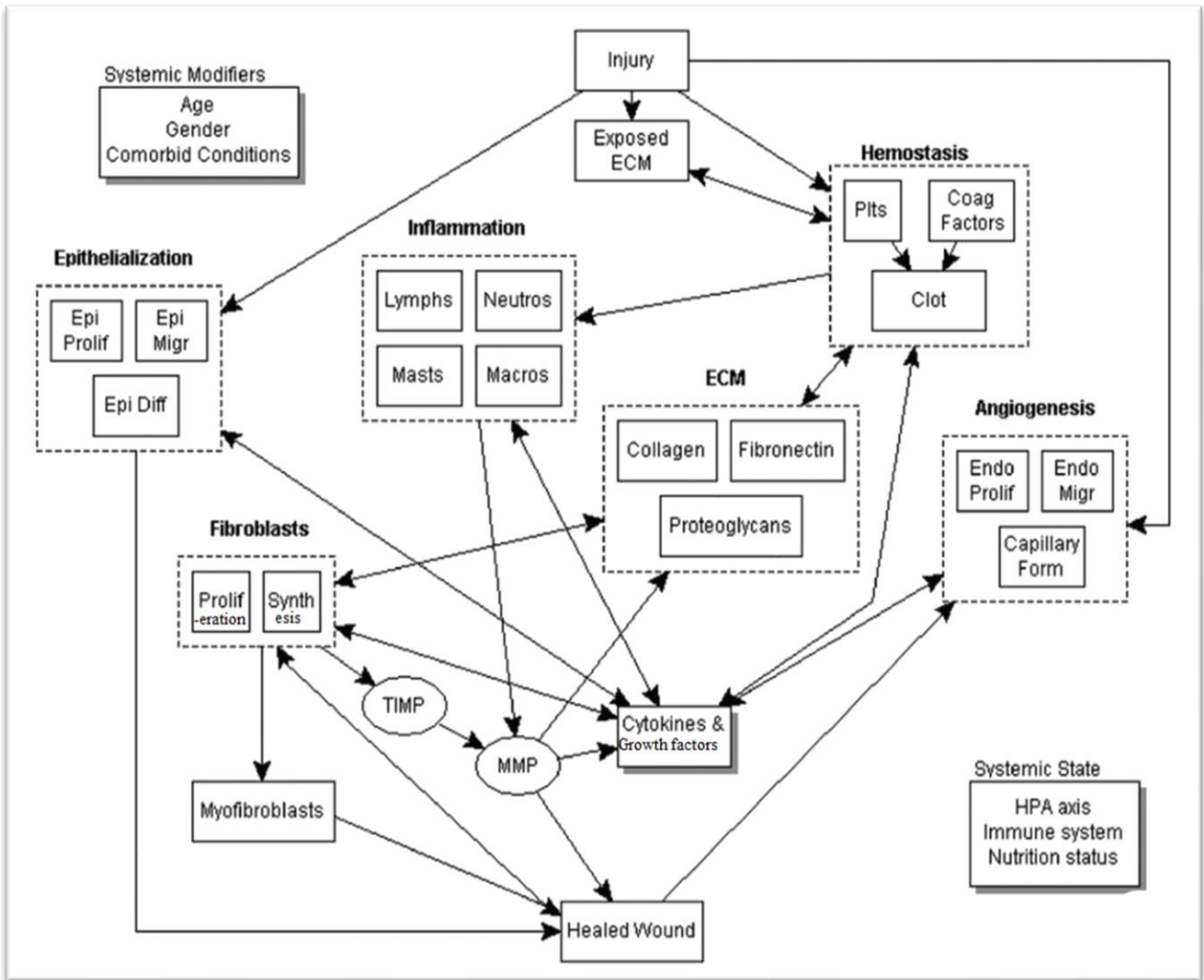


STAGES OF WOUND HEALING (FIG. 1)

Though the stages of wound healing can be divided into different phases, they are mostly overlapping. The first stage of wound healing is hemostasis followed by inflammation. The lesioned blood arteries constrict, and the leaked blood coagulates during a vascular inflammatory reaction, helping to maintain the vessel's integrity. The aggregation of thrombocytes and platelets into a fibrin network, which is the result of coagulation, depends on the activity of certain stimuli through the activation and aggregation of these cells. In addition to restoring homeostasis and acting as a barrier against microbial invasion, the fibrin network organises the temporary matrix required for cell migration, which in turn allows the skin to serve once again as a protective barrier and preserve the skin's integrity. The promotion of fibroblast proliferation and cell migration to the lesion's microenvironment are also made feasible by this (2). The proliferative stage's goal is

to create a stable epithelial barrier for activation of keratinocytes while reducing the size of the lesioned tissue region through contraction and fibroplasia. This stage, which involves angiogenesis, fibroplasia, and reepithelialization, is in charge of the lesion's actual closure. Within the first 48 hours following the formation of the lesion, these processes start in the lesion's microenvironment and can continue for up to 14 days (125).

### 1.3 COMPLEXITIES OF WOUND HEALING



COMPLEXITIES OF WOUND HEALING (FIG. 2)

## 1.4 FACTORS AFFECTING WOUND HEALING

Wound healing is prone to distress due to its complexity, and several factors can influence the healing process. This section will briefly discuss the impact of various variables on wound healing.

### **Local factors:**

1. **Infection:** Local infection is the most common problem that prolongs the healing process and distresses the process by delaying the inflammatory phase.

2. **Foreign bodies:** Foreign bodies (including nonviable tissue) are a physical obstacle to wound healing and a shelter for bacteria (mainly *Staphylococcus aureus*), prolonging the inflammatory phase. Wounds with foreign bodies are unable to constrict, resettle the region with capillaries, or epithelize fully (based on the size and region of the foreign body).

3. **Ischemia:** Ischemia can be described as the deficit of oxygen in certain body parts due to reduced blood flow in that area. Healing is an energy-dependent method that necessitates a sufficient supply of Adenosine triphosphate, the energy currency (ATP). The first anaerobic circumstances after damage encourage cells to switch to anaerobic ATP generation via glycolysis. Increased metabolism and protein synthesis define the proliferative phase of healing, which necessitates substantially more ATP via oxidative phosphorylation. Increased metabolism and protein synthesis define the proliferative phase of healing, which necessitates substantially more ATP via oxidative phosphorylation. This necessitates a plentiful blood supply to deliver glucose and oxygen. Hypoxia (low glucose) has the ability to stifle or even stop the healing process (7).

### **Systemic factors:**

A patient's traits may already lead to wound healing problems. Obesity, cardiovascular illness influencing tissue perfusion, a respiratory disease impacting appropriate blood oxygenation, metabolic disease, endocrine disease, and renal and hepatic failure are among these features.

1. **Diabetes Mellitus:** Increased blood glucose has a significant impact on wound healing; because of hyperglycemia's negative impact on molecular and cellular physiology, this is most likely a complex process. Extended hypoxia, which can be caused by both a lack of perfusion and a lack

of angiogenesis, is harmful to wound healing. Hypoxia can enhance the early inflammatory response, causing harm to the last longer by raising free oxygen radical levels (7, 8). When the formation of reactive oxygen species (ROS) surpasses the antioxidant capacity, hyperglycemia might exacerbate the oxidative stress (9). Hypoxia contributes to compromised healing of burn wounds. As the primary regulator of oxygen homeostasis, hypoxia-inducible factor-1 (HIF-1) is crucial predictor of healing outcomes. Throughout the healing process, HIF-1 plays a role in cell migration, cell survival under hypoxic circumstances, cell division, growth factor release, and matrix formation (10).

2. **Obesity:** Obesity is linked to an increased risk of various illnesses and ailments, including coronary heart disease, type 2 diabetes, cancer, hypertension, dyslipidemia, stroke, sleep apnea, respiratory issues, and delayed wound healing. During a hospital stay, obesity is a significant predictor of death and morbidity (11).

**1.5 BURN WOUND AND ITS TYPES:**

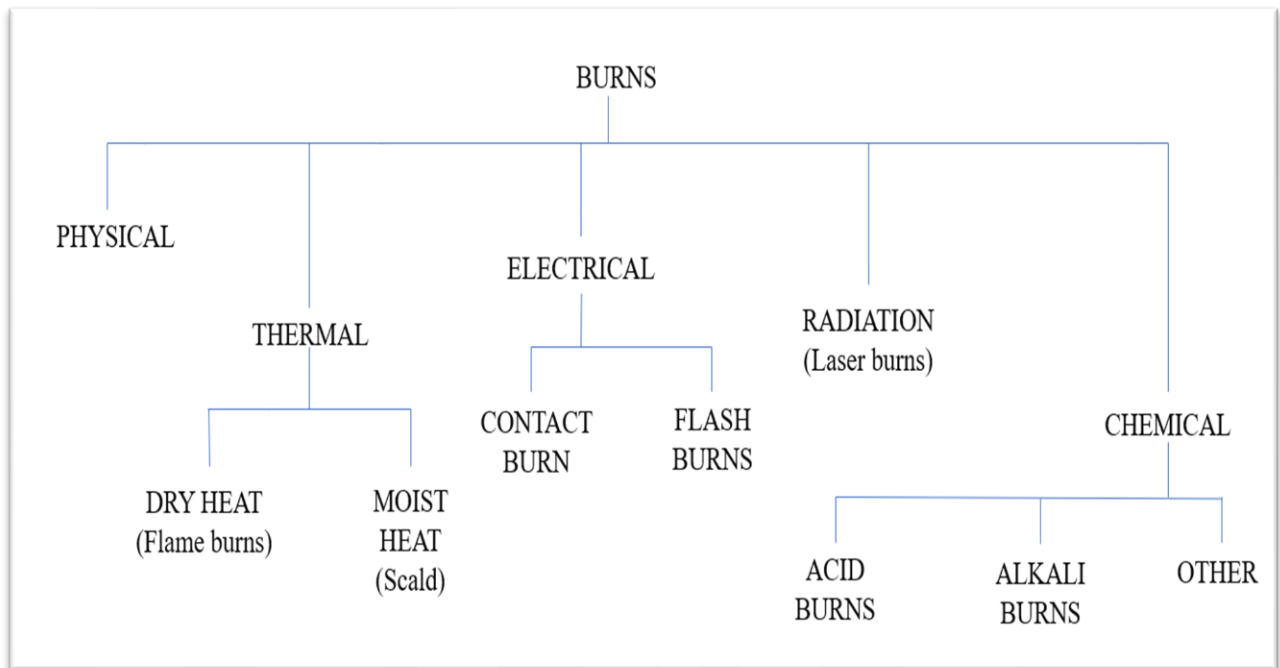


TABLE 1: TYPES OF BURN INJURY



Heat, cold, electricity, chemicals, radiation, or friction can all induce burn injuries. Burn injuries vary significantly in terms of the tissue injured, degree, and consequences. Because of nerve damage, muscle, bone, vascular, dermal, and epidermal tissue can all be affected, resulting in pain. A burn sufferer may suffer various possible deadly consequences, including shock, infection, electrolyte imbalances, and respiratory distress, depending on the location of the burn and the degree of the burn (12).

## **1.6 ANATOMY AND PHYSIOLOGY OF NORMAL SKIN:**

To better understand the classification of burn wounds, one must have a clear idea of the skin's structure.

The epidermis is the skin's primary and outermost layer. The epidermis is a stratified squamous epithelium with four to five layers, according to the location:

1. **Stratum Basalis (Basal cell layer):** This is the deepest layer and the one nearest to the dermis. It comprises melanocytes, a single row of keratinocytes, and stem cells and is mitotically active. Melanocytes are the cells that produce melanin, which is the pigment that gives our skin its colour. As keratinocytes from this layer migrate outward/upward to form the remaining layers, they develop and mature.
2. **Stratum Spinosum (prickle cell layer):** This layer makes up most of the epidermis and is made up of many layers of cells linked by desmosomes. Desmosomes allow cells to remain securely connected and structurally resemble "spines."
3. **Stratum Granulosum (granular cell layer):** This layer comprises many layers of cells with lipid-rich granules. As cells travel away from the nutrients in the deeper tissue, they start to immortalize, and cells become devoid of nuclei in this layer.
4. **Stratum Lucidum:** This layer, which contains primarily immortalized cells, can only be found in the thick skin of the soles and palms.
5. **Stratum Corneum (keratin layer):** This keratinized layer is the epidermis's outermost layer and functions as a protective coating. This layer helps in the management of water loss by avoiding internal fluid evaporation due to keratinization and lipid content.

The dermis is located beneath the epidermis, a dense layer of connective tissue made up of collagen and elastin that gives the skin strength and flexibility. Nerve endings, blood vessels, and adnexal structures, including hair shafts, sweat glands, and sebaceous glands, are all found in the dermis.

The papillary dermis comprises the apical layer of the dermis, which bends to produce papillae that protrude into the epidermis like small finger-like projections, and the reticular dermis is made up of the bottom layer of the dermis.

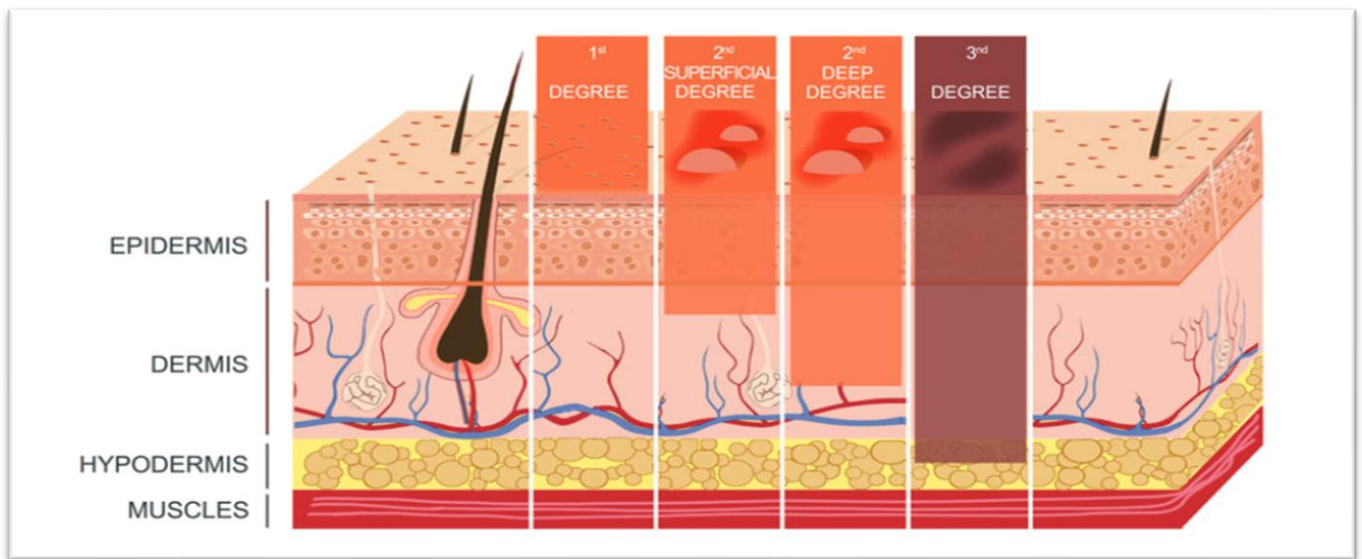
The hypodermis is the third and deepest layer of the skin, and it is primarily made up of adipose tissue.

**1.7 CLASSIFICATION OF BURN WOUNDS:**

The following are the different degrees of a burn wound based on how much skin and deeper tissues are involved:

Types of the burn wound	Condition of affected skin layers
First-degree burn wound	Skin is erythematic (absence of vesication)
Second-degree burn wound (Superficial)	Damages epidermis and only papillary dermis (vesication and inflammation present).
Second-degree burn wound (Deep)	Damages epidermis and deep reticular dermis (eschar is formed).
Third-degree burn wound	Full thickness burn wound involving epidermis, dermis, tendon, bones (eschar is formed)

TABLE 2: CLASSIFICATION OF BURN WOUND

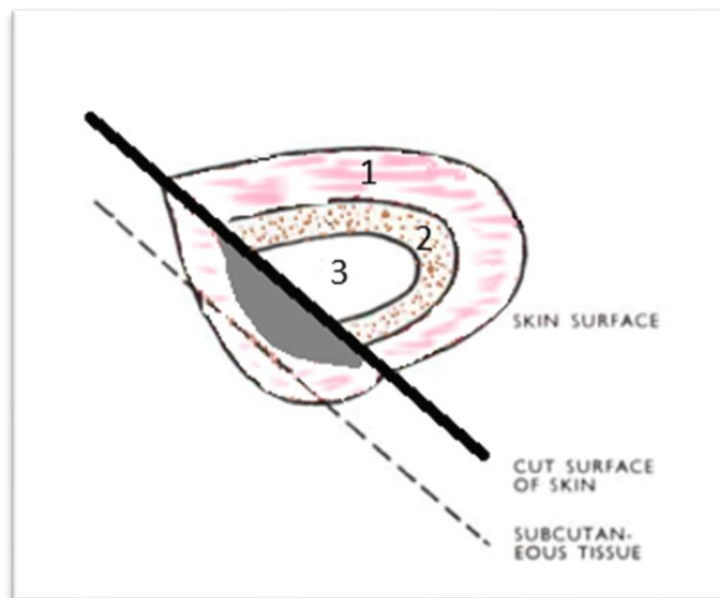


DEGREES OF BURN WOUND ALONG WITH STRUCTURE OF SKIN (FIG. 3) (126)

## 1.8 BURN WOUND MODEL:

Jackson (1959) has described three zones in the damaged burned tissue (16) During the first day after the injury, the burn is characterized by three concentric zones in the damaged area:

- **Zone of coagulation** – This is the central part of burns with complete coagulative necrosis, with the most amount of damage as of being exposed to the most significant amount of heat.
- **Zone of stasis**— The zone of stasis is at the periphery of the zone of coagulation. The circulation is sluggish in this zone, but it can recover after early and adequate resuscitation and proper wound care. (15)
- **Zone of hyperaemia** – This is peripheral to the zone of stasis. It results from intense vasodilatation, as seen in the inflammatory phase after the trauma. This eventually recovers completely. (4)



ZONE OF BURN WOUNDS (FIG 4)

The epidermis is capable of regenerative healing because it is derived from ectoderm. Deep dermal burns heal slowly, if at all, and depend mainly on migrating keratinocytes from surrounding intact skin. Keratinocytes which migrate from the skin bridges, fill up the interstices of meshed split-thickness skin grafts via this technique (17).

## **1.9 MECHANISM OF BURN WOUND HEALING:**

A severe inflammatory response follows a significant burn injury. Burn wounds may experience the effects of acute influx and inflammatory mediator and growth factor for a considerable time even though they are systemically transient. A burn site contains various cell types, including platelets, neutrophils, lymphocytes, macrophages, and fibroblasts. The activity of these cells is regulated by a complicated interplay between many cytokines and host neuroendocrine processes. The primary molecular regulators that control the genesis of the burn wound are vascular endothelial growth factor (VEGF), platelet-derived growth factor (PDGF), and transforming growth factor- $\beta$  (TGF- $\beta$ ). Transforming growth factor (TGF)-beta is necessary for the activation and proliferation of fibroblasts during the initial phases of wound healing. TGF-beta activity has been associated with deformity, ugly hypertrophic scars, and wound constriction. Treatment of a skin condition and, to some extent, restoration of the integrity, tensile strength, and barrier function of the skin are the goals of wound healing (18). If any of these steps, especially the inflammatory period, get elongated, the formation of a scar becomes high.

Damaged cutaneous blood vessels expose the platelets to ECM proteins which further enhances the process of rapid coagulation and formation of the fibrin clot (19). The diffusible chemicals released from platelets and mast cells like PDGF, and TNF transport the leucocytes to the wound (20,21). Diapedesis enables these cells to move from the peripheral circulation to the area of the wound (22). When the wound starts healing by passing the inflammatory phase, these inflammatory cells remove pathogens and debris from the wound while also beginning the healing and angiogenesis process.

During the next proliferative stage, a temporary wound bed is created by granulation tissue (GT) for the process of re-epithelialization. Additionally, neovascularization occurs to supply circulatory cells in the wound and support the newly formed tissue (23). Mast cells have been reported to accelerate the proliferation of fibroblasts, endothelial cells (ECs), and keratinocytes during the proliferative phase, which is necessary for the early closure of normal wound healing (24-27). Bidirectional interactions between keratinocytes and fibroblasts are necessary for the progression of wound healing.

Dermal wounds are frequently mended by collagen deposition and tissue remodelling, even though coordinated healing aims to restore tissue with a similar structure and equivalent functions to intact skin (28). The co-alignment of collagen bundles, the most abundant material of ECM and fibroblasts in GT, plays a crucial role in forming normal flat scars (29,30). For final wound closure, myofibroblasts exert contractile forces (31). After the completion of the wound closure, with the help of the contractile force exerted by the myofibroblasts, tissue remodelling occurs below the epidermal surface, and this process may take one year or more than that to complete (32).

### **1.10 MECHANISM OF ACTION OF METFORMIN IN BURN WOUND HEALING:**

The critical element of accelerated wound healing requires two events: polarisation of macrophages M1 to M2 phenotypes and a balanced amount of inflammatory cytokines. Studies have found that some multiprotein complexes come together as an inflammatory response and are called Inflammasome, within which NLRP3 is particularly interesting. NLRP3 inflammasome plays a vital role in the process of wound healing. Research shows that the absence of NLRP3 Inflammasome promotes the wound healing process while Metformin HCl can block the activity of this inflammasome (33). Recent studies also strongly suggest that blockade of the NLRP3 Inflammasome is crucial to accelerating wound healing in diabetic mice (34). The granulation tissue and collagen production were boosted by inhibiting the NLRP3 inflammasome-induced resolution of inflammation and hastening the re-epithelialization and wound closure process (35). Additionally, inhibiting the activation of NLRP3 inflammasomes encourages the polarisation of macrophages toward an M2 phenotype (36, 37). Previous research has suggested that activation of NLRP3 Inflammasome may be a factor in the slow healing of wounds in diabetes patients, whereas NLRP3 inflammasome negative regulation was suggested as a possible therapeutic target for enhancing wound healing. Importantly, topical administration of pharmacological inhibitors to mice's wounds, which can also suppress inflammasome activity, triggered a transition from pro-inflammatory (M1 macrophage) to macrophage (M2 macrophage) phenotypes and elevated levels of pro-healing growth factors. The number of cells producing the anti-inflammatory cytokines that reduce inflammation and the number of cells secreting the growth factors required for proliferation, migration, and the healing process both rise as the number of M2 macrophages in wounds increases (38, 39, 40). There are some instances where studies show that the absence of NLRP3 Inflammasome can reduce the M1 phenotype, which prevents fibrosis in the kidney (41).

It has been found that the NLRP3 Inflammasome activates caspase-1, which induces the cleavage of (IL)-1  $\beta$  and -18 into their active forms. Excessive formation of these two interleukins leads to fibrosis. Along with that, this dysregulation also enhances excess keratinocyte formation, which can lead to scar formation (42). Metformin significantly regulates the AMPK/mTOR/NLRP3 inflammasome signaling pathway (33). Study shows that this potent AMPk activator (43,44) also boosts macrophage polarization, which is necessary for accelerating the wound-healing process by intracellularly delivering ATP to wound tissue. This novel ATP-mediated acceleration arises due to an alternative activation of the M1 to M2 transition (macrophage polarization), a central and critical feature of the wound-healing process. This M2 macrophage helps increase the amount of pro-inflammatory cytokines like TNF, IL-1 beta, IL-6, and Vascular Endothelial Growth Factor (45). These factors are important for boosting angiogenesis in the damaged area by promoting neovascularisation and production of granulation tissue (GT) for hastened wound recovery (33,46).

# LITERATURE REVIEW

## LITERATURE REVIEW:

- Birch et al. studied on hard and soft pectin hydrogels and their effect on repairing tissue damage and acute inflammation. The formulations made by pectin were biodegradable in nature and can contribute to formation of new connective tissues and collagen fibres. They showed Pectin significantly has an anti-inflammatory effect along with the potential of formation of collagen fibres on the surface of hard pectin hydrogel (47).
- Shahzad et al. used pectin along with the sodium alginate to form crosslinked films for preparation of sustained release formulation of Cefazolin for treatment of burn wounds and the important reason to use this in the film was to make it biodegradable and biocompatible in nature. The drug was incorporated into chitosan nanoparticles for obtaining a sustained delivery into the site of wound. The formulation was optimized by different characterization such as measuring the particle size, entrapment efficiency and zeta potential along with assessment of physical and chemical properties of the film like WVTR, swelling index, FTIR and DSC. The scientists also reviewed that a moist approach could keep the wound hydrated and this is better than the dry approach and it enhances the formation of epithelial skin layer (48).
- Hydrogels were formed by acrylamide and maleic acid using different monomer ratios using PEG 400 as a non-toxic crosslinker by Kaşgöz et al. and it was found out by them that PEG 400, which has a good elasticity and long chain structure, can be used as a crosslinker instead of (NMBA)N, N'-methylenebisacrylamide, the classic crosslinker (49).
- Winter tried to study about the approach between dry and wet, and he concluded that keeping the wound area moist enhances the rate of epithelization twice as much as applying dry formulation into the wound and showed that formation of dry scab retards the process of wound healing (50).
- Dyson et al. showed the comparison between the wet and the dry approach and they showed the result that wet approach is better than the dry one, as vessel number, angiogenesis must be found more in case of wet approach (51).
- Demling et al. studied about the side effects of silver nitrate solution. They reviewed that silver solution alone is not that harmful to the wounds, but their salts are. Silver nitrate solution is harmful to the damaged area as they contain nitrate which is a potent oxidizing agent and it potentially retard healing (52).



- Monafio and West showed in their studies that silver sulfadiazine has a side effect like leucopenia, which happens within 2 to 3 days of the initiation of silver sulfadiazine therapy and the neutrophil count decreases. When the therapy is withdrawn, the neutrophil count tends to increase after some days (53).
- Klasen reviewed about some side effects of use of silver nitrate solution in burn wound. One of the drawbacks is the black staining of the drug, as silver nitrate is photosensitive in nature. Another one is the decreasing value of serum sodium and chlorine. Moreover, elevated silver level was found the different organs of the body (54).
- Monsuur et al. studied whether eschar formation has a positive or negative impact on the early healing process of burn wounds by collecting the burn wound extract as it contains a perfect amount of cytokines and chemokines. Study shows that the formation of eschar is a positive sign in the healing process as granulation tissue formation proceeded rapidly as long as the eschar was kept, and after its removal (escherectomy), an excessive amount of granulation tissue got formed, which led to scar (55).
- Zhang et al. found that if PGE2 is released for a prolonged period, it enhances the polarization of M2 macrophages. This process can reduce inflammation and boost angiogenesis, which is an incredibly positive sign for the wound healing process (36).
- He et al. reviewed that an increase in the amount of IL-33 can effectively reduce the wound size while amplifying the number of M2 macrophages both in in-vitro and in-vivo conditions.
- Qing et al. studied the effect of topical application of metformin in burn wounds and described the potential pathway to how metformin worked for accelerated wound healing. Metformin, the most used first-line antidiabetic drug, is often given to burn patients to reduce their sudden hype of blood sugar levels after burn injury. The topical application of this drug worked through AMPk/mTOR/NLRP3 signaling pathway while it also induced the polarization of M2 macrophage, one of the most important factors contributing to accelerated wound healing (33).
- Jeschke et al. studied in their paper that metformin is the first choice of antidiabetic drug to be given to a patient having severe burn injury. It has equal effectiveness to insulin and does not cause hypoglycemia in the patient. Moreover, it also improves the condition of insulin resistance (56).

- Border and Ruoslahti reviewed the dark side of the growth factors. They showed that TGF beta though beneficial for the formation of the extracellular matrix after injury, by the induction process and attracting more growth factors along with inhibiting the proteases; but this induction process only leads to scar formation. The excess accumulation of TGF $\beta$  enhances the complexity of the wound by making it chronic and generating scar tissue (57).
- Gilani et al. followed the solvent casting method to prepare nanocomposite films using the three components PEG 400, chitosan, and the drug. In this method, the mixture of the components like polymer and others was prepared by constant agitation using a magnetic stirrer and then poured into plates. It was then allowed to dry by evaporation of the selected component (58).

# AIM AND OBJECTIVE

**AIM:**

This project aims to prepare a biodegradable and biocompatible film by incorporating metformin into a matrix formed by crosslinking two polymers, Pectin and Carbopol, adding flaxseed gel to enhance the rate of burn wound healing.

**OBJECTIVE:**

- To suggest the calculated ratio of the polymers (Pectin and Carbopol) at an optimum amount, making the film biodegradable and biocompatible and ideally making it bio adhesive.
- To provide an excellent moisturizing effect to satisfy the wet approach towards healing the burn wound.
- Standard dressings available in the market irritate the skin at the time of removal on the following day as it adheres to the skin tightly. To prevent this much adhesion, a biodegradable film can work well by keeping the wound exudates preventing deep infection along with providing the drug evenly, and later it can be easily removed.
- To evaluate the following characteristics of formulation like moisture content of formulation, swelling index, entrapment efficiency of the drug, in vitro drug release study, morphological studies, and analytical studies to find out drug-polymer interactions.
- To conduct *In-vivo* studies and check the rate of wound contraction in *In-vivo* models.

# EXPERIMENTAL

## **4.1 EXPERIMENTAL:**

All the chemicals used in this experiment were of analytical grade. Pectin and Carbopol were purchased from Himedia Laboratories Pvt. Limited, Mumbai, India. PEG 400 and Glycerol were bought from Merck Specialties Private Limited, Mumbai. Flaxseed was purchased from the market. Deionized water was used for all the analyses done. Metformin was received as gift sample from C.I Laboratories(56/1, Room No.d/13, 2nd Floor, B R B Bose Road, Kolkata, West Bengal 700001), India.

### **4.1.1 Reagents and Materials:**

#### **4.1.1.1 Pectin:**

Pectin is an anionic heteropolysaccharide obtained from the terrestrial plant cell walls (60,61,62). Pectin is a natural hydrocolloid, non-cytotoxic, biocompatible, and biodegradable, making it appropriate for using in wound healing procedures. Because the backbone chain contains hydroxyl, carboxyl, and carboxymethyl groups, it is easily functionalized and modified (62). Pectin and its derivatives are believed to be highly effective for wound healing applications as it has a strong anti-inflammatory effect (63) which is highly desirable in treating burn wounds and chronic diabetic wounds. Pectin's potent anti-inflammatory activity, which reduces inflammatory enzymes like iNOS and COX-2, is caused by the high number of esterified galacturonic acid residues in the substance (62, 64).

#### **4.1.1.2 Carbopol:**

Carbopol is used as a thickening agent in this formulation and also as a component of film as it can provide the desired viscosity and is also nontoxic (65). According to certain research studies, Carbopol-containing scaffolds can promote fibroblast adhesion and growth and influence cell migration (66, 67, 68). Additionally, carb hydrogel has shown the suitable ability for full thickness wound healing and continuous release of curcumin as a drug (68). High water affinity, rapid swelling, high viscosity, intriguing bio adhesive, and rheological characteristics, high absorption capacity, minimal toxicity, and adequate biocompatibility are only a few of the distinctive qualities of the network formed by carbohydrate gels. Because of these characteristics, carb is a suitable medication retaining substance for wound healing (69, 65).

#### **4.1.1.3 PEG -400:**

It is used in the formulation as a crosslinker (70, 49), also to get the desired property of the film as soft, elastic, and flexible (71).

#### **4.1.1.4 Flaxseed gel:**

Flaxseed mucilage, along with the proteinaceous part, was extracted and added to the formulation to enhance the wound healing property and provide good moisture content in the damaged area. Flaxseed's triglycerides and fatty acids can improve skin hydration by lowering trans-epidermal moisture loss (72, 73). According to Cunnane et al. (1993), flaxseed oil contains around 73 percent polyunsaturated fatty acids, of which omega-3 polyunsaturated fatty acids have been shown to boost the production of pro-inflammatory cytokines at wound sites and thus speed up the healing of skin wounds (74). In addition, it is abundant in fatty acids such as oleic, linoleic, palmitic, and stearic acids, as well as linolenic acid, which accounts for 39–60% of its total fatty acid content (75). Oleic, linoleic, and linolenic acids provide cells with the lipids they need for respiration and membrane repair (76,59).

#### **4.1.1.5 Glycerol:**

It was added to retain moisture in the formulation (77) as it is one of the effective humectants. Its high degree of hydroxyl groups helps it to retain water and moisture, which is desirable for burn wounds (78).

#### **4.1.1.6 Metformin:**

Metformin is a biguanide drug that increases circulatory glucose absorption by improving insulin sensitivity in a cell-specific way while inhibiting hepatic glucose synthesis (3). India is now referred to as "the diabetes capital of India," and this is not just any hype created by the media; India has the highest proportion of diabetic patients. It is obtained from the French lilac *Galega officinalis*. Metformin treatment reduces hepatic glucose synthesis, boosts insulin receptor tyrosine

kinase activity, and improves insulin sensitivity in muscle and the liver (79,80) . The way metformin works depends on the cell type and tissue. Metformin boosts the mitochondria's oxidation and absorption of glucose and fatty acids in skeletal muscle. (81). In the liver, Metformin decreases lipid synthesis and gluconeogenesis while decreasing fatty acid production and lipolysis (81). By turning off beta cells in the pancreas, Metformin decreases the amount of insulin secreted. Metformin decreases fatty acid oxidation by suppressing Srebp1c expression to prevent steatosis brought on by a high-fat diet (82).

The most well-known effect of Metformin is its ability to increase insulin sensitivity by activating canonical AMPK and Akt signaling in muscle cells through atypical protein kinase C (PKC) activation, which causes GLUT4 membrane translocation for glucose absorption (79, 83, 84,85). Metformin predominantly inhibits mitochondrial complex 1 and upregulates the alpha subunit in human hepatocytes, which reduces glucose synthesis(86). Metformin likewise impacts other signaling pathways in the diverse cell and tissue types. Metformin decreased Akt phosphorylation and phosphatase and tensin homolog (PTEN) expression in 3T3-L1 preadipocyte cells in an AMPK-dependent manner while increasing the phosphorylation of JNK and mammalian target of rapamycin (mTOR). Loss of PTEN expression elevated JNK and mTOR and recovered insulin induced Akt phosphorylation (80). Biguanide therapy of primary hepatocytes prohibited glucagon signaling through AMP buildup and cAMP suppression, decreasing protein kinase A (PKA) signaling and gluconeogenesis (87). Even though Metformin affects diverse cell types in various ways, the mitochondrial respiratory complex I is a route that is virtually universally suppressed in research (3).



## **4.2 METHODOLOGY:**

### **4.2.1 Preparation of the flaxseed gel:**

Flaxseeds were bought from the market, appropriately washed, and kept for air drying. Within a clean mixer grinder, it was coarse ground. After that, the powdered flaxseed was taken, and 1.5g was weighed. 10ml of deionized water was mixed and subjected to heat for 15 to 20 minutes. The mixture was constantly stirred while heating, and the consistency was checked. When it started to get thicker and the gel-like consistency appeared, the heat was turned off and given time to cool down. A clean muslin cloth was taken and kept in UV for 10mins. The gel was passed through a UV sterilized cloth to get a clean texture. It was collected in this manner to obtain the mucilage along with the proteinaceous part.

### **4.2.2 Preparation of the formulation:**

Pectin, one of the polymers to be used in the formulation, was taken in definite quantity, mixed with deionized water, and placed in a magnetic stirrer (REMI Lab Stirrer, India) for constant stirring at 600 to 700 rpm. When it was almost dissolved, a certain amount of Carbopol was added to the mixture and allowed continuous stirring at the same rpm for 60 to 90 minutes to avoid bubble formation. Pectin and Carbopol were taken in different ratios like 1:1, 2:1, and 3:1 and named as F1, F2 and F3 respectively. As Carbopol is very much hygroscopic and has a suitable thickening property, its quantity was kept constant the amount of pectin was changed every time in different formulations to check its credibility. After the formation of the mixture of Pectin and Carbopol, the flaxseed gel was added to it and allowed for stirring for up to 10 minutes. PEG 400 (Polyethylene Glycol) was added to the mixture as a crosslinker (49). After 5 to 10 minutes, Metformin was weighed, added to the solution, and continuously stirred (REMI Lab Stirrer, India). At last, 4 to 5 drops of glycerol were added to every 10ml of the solution while stirring. Finally, the homogenous mixture was poured into clean Petri dishes following the solvent casting method (58). It was then kept in an incubator for 48 hours and abraded.

## **4.3 OPTIMISATION**

### **4.3.1 Physical Characteristics**

Metformin-loaded Carbopol – pectin-based films were characterized in terms of weight uniformity. Briefly, the size of 2.0 cm × 2.0 cm of 3 films were cut accurately and weighed on electronic balance (Shimadzu, Japan) to calculate the mean weight. The thickness of formulated films was measured using an electronic micrometer (U-Therm, China) according to Patel et al. described method. The result was expressed in a triplicate manner (measurements ± standard deviation) (88).

2×2 cm<sup>2</sup> films were cut from different areas of each of the films F1, F2 and F3, and the weights were measured, and the uniformity was calculated.

### **4.3.2 MOISTURE CONTENT STUDY:**

Moisture content study was performed by taking the initial weight of the film ( $W_i$ ) film was put in a hot air oven at 90°C for 24 hours and kept in a desiccator for three consecutive days to lose the maximum moisture. The final weight ( $W_f$ ) was measured in a triplicate manner, and their mean value was taken. The following formula is used for the calculation (91)

$$MC = 100(W_i - W_f) / W_i$$

### **4.3.3 Water solubility study:**

2×2 cm<sup>2</sup> portion was cut from the film and separated. This portion of the film was dried at 95°C for 24 hours in a lab oven. The weight was measured initially in this stage. (Initial weight=  $W_i$ ). After that, it was immersed in 100 ml of deionized water and kept for stirring in a magnetic stirrer for 8 hours at 25°C. The solution was passed through Whatman filter paper(Grade-1) (91). The insoluble portion on the paper was dried at 110°C (until it reached constant weight) and noted as  $W_f$ .

$$WS \% = [(W_f - W_i) \times 100] / W_f$$

#### 4.3.4 Transparency measurement:

Rectangular pieces of each film (40×20 mm) were cut. In the UV spectrophotometer (Shimadzu, Japan) where an empty cell was taken as reference, and the pieces of films were placed in the test cell, and their absorbance was measured at 500 nm. This process was repeated three times, and their mean was calculated (91).

Opacity= absorbance at 500 nm × Film thickness

#### 4.3.5 Water Vapour permeability:

The WVTR test was performed using the upright wet cup method according to the JIS 1099A standard (88, 92). The moisture permeability of the Pectin-Carbopol films (F1, F2, F3) was evaluated by determining the water vapor transmission rate across the films. A circular piece of the specimen was affixed over the top of a permeability cup of 6 cm in diameter, having 50 g of CaCl<sub>2</sub>, using parafilm (water resistant tape) to avoid any moisture loss through the edges. The cup was then placed in an incubator at 90 ± 5% RH at 40 ± 2 °C. The following formula calculated the WVTR:

$$\text{WVTR}=(W_2-W_1 \times 100)/S \text{ g/m}^2/\text{day}$$

$W_1$  and  $W_2$  are the weights of the permeability cup at the end of the 1st and 2nd hour, respectively, and  $S$  is the area of the hydrogel films.

#### 4.3.6 Swelling index:

The film was cut into a 1.5×1.5 cm<sup>2</sup> segment, and its dry weight was measured ( $W_{\text{dry}}$ ) properly. The cut part was dipped in 30 ml of deionized water and incubated at 37±2°C for 30 mins. After that, it was removed from the water, and the wet weight was determined ideally. A filter paper was used to blot and remove the excess water from the film (88). The swelling index was calculated by using the following formula:

$$\text{Swelling index}=(W_{\text{wet}}-W_{\text{dry}})/ W_{\text{dry}} \times 100\%$$

#### **4.3.7 Dehydration rate:**

At first, the test solution was prepared by taking 1.149g Sodium Chloride and 0.184g Calcium chloride dihydrate in 500ml deionized water. The solution was warmed to 37°C. 0.5× 0.5 cm<sup>2</sup> film was cut, and the weight was measured. The cut film was dipped in the warm test solution and placed in an incubator for 30mins at 37±2°C (according to body temperature). The weight was measured (B). Then it was removed from the incubator and suspended by a tweezer in one corner and allowed to drip off to lose the excess solution for 30 seconds. Then again, it was placed in Petri dish and kept for 24 hours at 37±2°C in the incubator and reweighed (A)(93).

Mass loss upon drying (%) =[(B-A)×100]/B

#### **4.3.8 Rate of absorption:**

A drop of test solution was put on the film's surface using a dropper, and it was allowed to get absorbed. The time taken for this method is measured in seconds. Now, 20 drops were placed on five such films, and the mean of their absorption time was calculated (88).

#### **4.3.9 *In-vitro* Drug release:**

Preparation of standard solution:

100 mg Metformin was weighed and transferred into a 100ml volumetric flask. The drug was dissolved into 40 ml of distilled water, then the volume was made up to the mark, and the final concentration of the solution was 1000 µg/ml of Metformin Hydrochloride (94).

Preparation of working standard:

Aliquots were drawn from the stock solution and diluted with a sufficient amount of distilled water to obtain the desired concentration, and the absorbance values of different concentrations were measured at 231 nm.

Drug release profile from the formulation:

2×2 cm<sup>2</sup> was cut from each of the films of known thickness having a different ratio of Pectin and Carbopol like 1:1, 2:1, and 3:1. The in vitro release study was conducted in a phosphate buffer medium (pH 7.4) using a Franz diffusion cell (124) at 37°C ± 2°C with continuous stirring at 50 rpm speed placed on a magnetic stirrer. Drug solubility in the release media is necessary for its transportation through the dialysis membrane. At predetermined intervals like 15 minutes, 30 minutes, 1 hour, 2 hours, 3 hours, and 4 hours, 1 ml sample was withdrawn and replaced with a fresh dissolution medium to maintain sink condition. The samples were diluted and filtered, and the drug contents were determined UV – Vis spectrophotometer (Shimadzu, Japan) at 231 nm. The in vitro drug release data were plotted using kinetic models like zero order, first-order, Higuchi, and Korsmeyer-Peppas to predict the drug release kinetics.

#### **4.3.10 DRUG ENTRAPMENT EFFICIENCY:**

The total drug content in microspheres was determined by the method described by *Patel et al., 2018* (88). 2×2 cm<sup>2</sup> of the films were cut from the F1, F2, and F3 formulations dipped in phosphate buffer pH 7.4 and kept aside for 24 hours at 40°C. Then the sample was sonicated (Digital Ultrasonic Cleaner, Equitron PVT. LTD., India) for 15 minutes. After that, the aliquot was taken from the supernatant and analyzed using a UV spectrophotometer (Shimadzu, Japan) at 231nm . The following formula calculated the percentage of encapsulation efficiency,

$$\% EE = \frac{ED}{AD} \times 100$$

Where % *EE* is the percentage encapsulation efficiency, *ED* is the amount of encapsulated drug, and *AD* is the amount of added drug.

#### **4.3.11 FT-IR spectral analysis**

The FT-IR spectra of Metformin and individual components like Carbopol, pectin, and optimized formulation were analyzed by FT-IR spectrometer (Shimadzu FTIR-8400S) in the range between 4000 - 500 cm<sup>-1</sup> at a resolution of 4 cm<sup>-1</sup> with a scan speed of 1 cm/s to assess the chemical composition and probable interactions between the polymers and drugs in formulated optimized films (89).

#### **4.3.12 SEM studies:**

The film's surface morphology was carried out by scanning electron microscope (SEM) (Model: ZEISS EVO-18). The sample was examined after coating with platinum by a fine auto coater operated at an acceleration voltage of 15Kv under ambient conditions (88).

#### **4.3.13 XRD Analysis:**

X-ray diffraction (XRD) analysis was performed for the mixture of the raw materials and the powdered drug with Cu-K $\alpha$  radiation source ( $\lambda = 1.5406 \text{ \AA}$ ) at 25 °C operated at 40 Kv and 40 mA, using a 0.02° step size and 2 $\theta$ /min scan speed (90).

#### **4.3.14 Differential Scanning Calorimetry studies:**

Differential scanning calorimetry (DSC) studies of Metformin and optimized formulation (F<sub>3</sub>) were performed to assess the thermal stability of the film. Briefly, 2 mg of samples were taken in a DSC sample holder, and calorimetric curves were recorded in the range of 25 - 350° C at a heating rate of 10° C/min under a nitrogen environment (50.0 ml/min) by using Differential Scanning Calorimetry (Shimadzu DSC-60 Systems, Japan) (88).

### **4.4 IN-VIVO STUDIES:**

#### **4.4.1 Animals and ethics statement:**

Adult male Wistar rats weighing 150 $\pm$ 20 g, used in the current study were obtained from M/S CHAKRABORTY ENTERPRISE Regd.No. 1443/PO/Bt/s/11/CPCSEA. The animals were accommodated separately in a temperature-controlled room with a 12:12 h light-dark cycle (Lights turned on at 7 AM) under standard laboratory conditions (room temperature 25°C  $\pm$  2°C and 60 $\pm$  10% RH) with free access to rodent diet and water. All procedures involving animals and their care in the present research work were performed consistent with the guidelines arranged by the IAEC of the Department of Pharmaceutical Technology, Jadavpur University (JU/IAEC-22/09).

#### **4.4.2 Creation of burn wound model:**

The burn wound was created following the method described by *Venter et al., 2015* (96) with little modifications. The animals were anesthetized with xylazine (7.5–10.5 mg/kg) and ketamine (50–70 mg/kg). The skin of the dorsal area (interscapular region) was shaved, followed by cleaning, and disinfecting with the beta-dine solution, and then burn wounds (in a total area of 3.8) were created by applying heat on the skin for 10 seconds with a soldering iron dice with a diameter of 2 cm previously heated in boiling water for 20 minutes. All animals were resuscitated instantly with an i.p. injection of lactated Ringer's solution (2 ml/100 g body weight). Until the conclusion of the research period, rats were kept in individual housing. Each rat received one burn on its dorsum(95).

#### **4.2.3 Experimental design:**

Eighteen male Wistar rats (150±20 g, nonfasted) were randomly divided into four groups. One group containing three animals was kept in healthy condition with proper diet and water, and all other groups contained five animals each. The control group received no treatment; one group was treated with silver nitrate gel, and another was treated with the optimized formulation. Treatments were carried out every 24 hours for 12 days. The eschar's fall was considered the complete re-epithelization, and the digital photographs were taken and laid on the scale to assess the wound contraction rate (97).

The wound contraction rate was calculated by the formula =  $(W_i - W_f) / W_i \times 100\%$

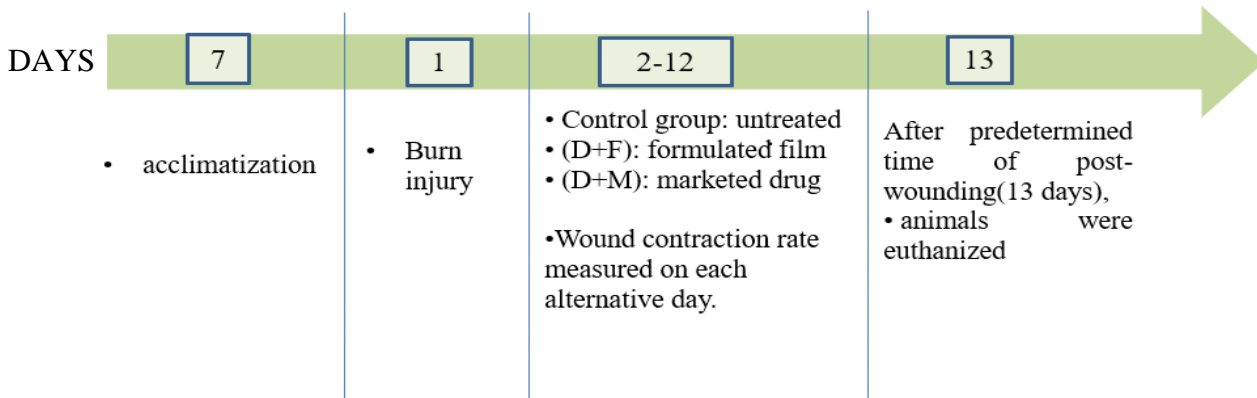


FIG. 5: STUDY PROTOCOL

Sl. No.	Groups	Animal Species	No. of animals
1	Naïve	Wistar Rats	3
2	Disease group		5
3	Disease + Metformin Film (F1)		5
4	Disease + Silverex		5

TABLE 3: EXPERIMENTAL GROUPS OF ANIMALS



# RESULTS

### 5.1 Physical Characteristics:

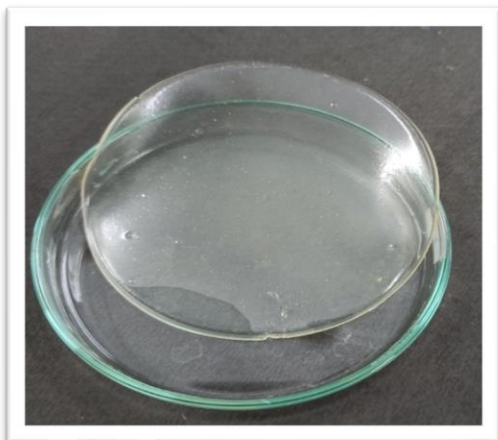


FIG. 6

The film was strong enough to be peeled off from the petri dish confirming a good tensile strength. Overall, the surface of the optimized film was smooth, and it showed adhesiveness to the skin. Thickness of the films was in the range of 0.28 to 0.34 mm as measured from different portions of the film. The weight was measured from cutting different portions of same size from films in a triplicate manner and taking the mean. The average weight of the cuttings was  $0.0776 \pm .003$  g, proving the weight uniformity of the films. Figure 6 represents a

picture of Metformin loaded Pectin-Carbopol film.

### 5.2 Moisture content study:

As the initial and final weight of the film came to be 3.4276g and 1.7983g, following the formula, the film's moisture content was  $47.53\% \pm 5\%$ . Minoura et al. stated in their research work moisture content of film were between 20 to 40% which was optimal for treating burn wound in their project. As this film was a wet approach for recovery of the burn wound, this moisture content of the film gave satisfactory results. Different approaches were taken to obtain the desired moisture content of the films. For this, a variable amount of Pectin and crosslinker PEG 400 were used. In the case of these approaches increasing the amount of crosslinker, increased the requirement of water to be added to the formulation, which led to a deformed film. An increase in pectin did not affect the moisture content study, and the result was almost identical to the optimized formulation (103).

### 5.3 Water solubility study:

The initial weight of the  $2 \times 2$  cm<sup>2</sup> cut film after drying for 24 hours was 0.0340g. After immersing it in water and stirring for 8 hours, the final weight obtained after passing that solution through the

Whatman filter paper and drying was 3.8235g. According to the formula, the water solubility of the film came to 99.11% (88).

#### **5.4 Transparency measurement:**

The absorbance value of the film was measured at 500 nm while an empty cell was taken as reference. Film thicknesses were measured in triplicate, and the mean was in the range of 0.28-0.34 mm, measured from ten random positions. The films' transparency ranged from 1.2 to 3.67. According to the accepted norm,  $E = 1.2$  denotes a more transparent film, and  $E = 3.67$  a less transparent film. As a result, the transparency of the film F3 was higher, and F1 had the lowest value of transparency, which showed that the addition of pectin increased the transparency (123).

#### **5.5 Water Vapour Permeability:**

Results show that permeation cups have an adequate amount of anhydrous Calcium Chloride and maintain negligibly low and constant headspace humidity. In contrast, the weights of the permeability cups were measured at the end of the first and second hours, and the Water Vapour Permeability Rate of the optimized film came from  $1989 \pm 137 \text{ g/m}^2/\text{day}$ . While other two films, F2 and F3, have lower permeability rates of  $167 \pm 112 \text{ g/m}^2/\text{day}$  and  $50 \pm 27 \text{ g/m}^2/\text{day}$ . Patel et al. confirmed that wound dressings having Water Vapour Permeability Rate near about 2000–2500  $\text{g/m}^2/\text{day}$  are suitable for the healing process as they can inhibit the excessive loss of moisture from the wound, providing a moist approach, but at the same time not too high to accumulate the wound fluid which may lead to further infection. (88) From the result, it can be understood that the addition of pectin increases the WVTR (104).

#### **5.6 Swelling index:**

The swelling index of the optimized film F1 was lesser than other formulations, F2 and F3. It was observed that an increase in the amount of Pectin increases the swelling capacity of the formulation at phosphate buffer pH 7.4. Moreover, flaxseed gel in the formulations attracted to water, which

increased the swelling capacity of all the films, whereas the addition of glycerol to the formulations also contributed to it (88). The values are provided in Table 3.

### **5.7 Dehydration rate:**

Optimized film F1 has a dehydration rate of around  $83\pm 4\%$ , while F2 and F3 have a much lower rate of dehydration as more pectin present in the films prevented the film's moisture loss. It was calculated after keeping all the moist films in an incubator for 24 hours (88).

### **5.8 Rate of absorption:**

Simulated wound fluid was dropped on the film's surface to check the films' absorption rate. Results show that the optimized film's absorption rate was lower than the other two. The probable reason for this is due to less amount of pectin in the films. The pectin amount was higher in F2 and F3, so it attracted moisture quickly. So, the first drop of wound fluid took only  $5\pm 2$  seconds to get absorbed into all of the films. However, the result varied in the second step of putting twenty drops of wound fluid and showed quick absorption in the case of F2 and F3. F2 and F3 respectively took 51 and 53 seconds to absorb, while the time taken for F1 was longer that is 67seconds (88).

### **5.9 *In-vitro* drug release studies:**

The drug was released from formulated films in phosphate buffer (pH 7.4) at regular time intervals. The results indicated that the drug release rate from the optimized formulated film was minimum at 15mins while gradually increasing with time. This study exhibited that the release of the Metformin in the physiological environment is due to the polymeric chain relaxation. As the aqueous solvent starts to imbibe the film, the polymeric chain relaxes the drug molecules into the solvent with time (105). The percentage of drug release from the optimized film F1 was  $84.61\pm 2.69\%$ , while release from F2 and F3 were respectively  $14.70\pm 5.61\%$  and  $22.61\pm 7.12\%$ . As the figure 7 shows that F1 has shown a controlled release, whereas F2 did not release the drug properly into the solvent, and F3 also did not constantly release the drug; instead, it was released at the end of four hours in a sudden anomalous manner, which is not desired at all. So, the Drug release

kinetics study was examined for the optimized formulation F1 by curve fitting method according to zero order (8a), first order (8b), Higuchi model (8c) and Korsmeyer-Peppas's Model (8d). It has been observed that the release of Metformin from the formulated film(F1) followed Higuchi model kinetics derived from the correlation coefficients of the different kinetics models. The highest value of the regression coefficient was considered as the best fit, resulting in the Higuchi model suggesting a constant and controlled release of the drug from the polymeric matrix by diffusion method without erosion.

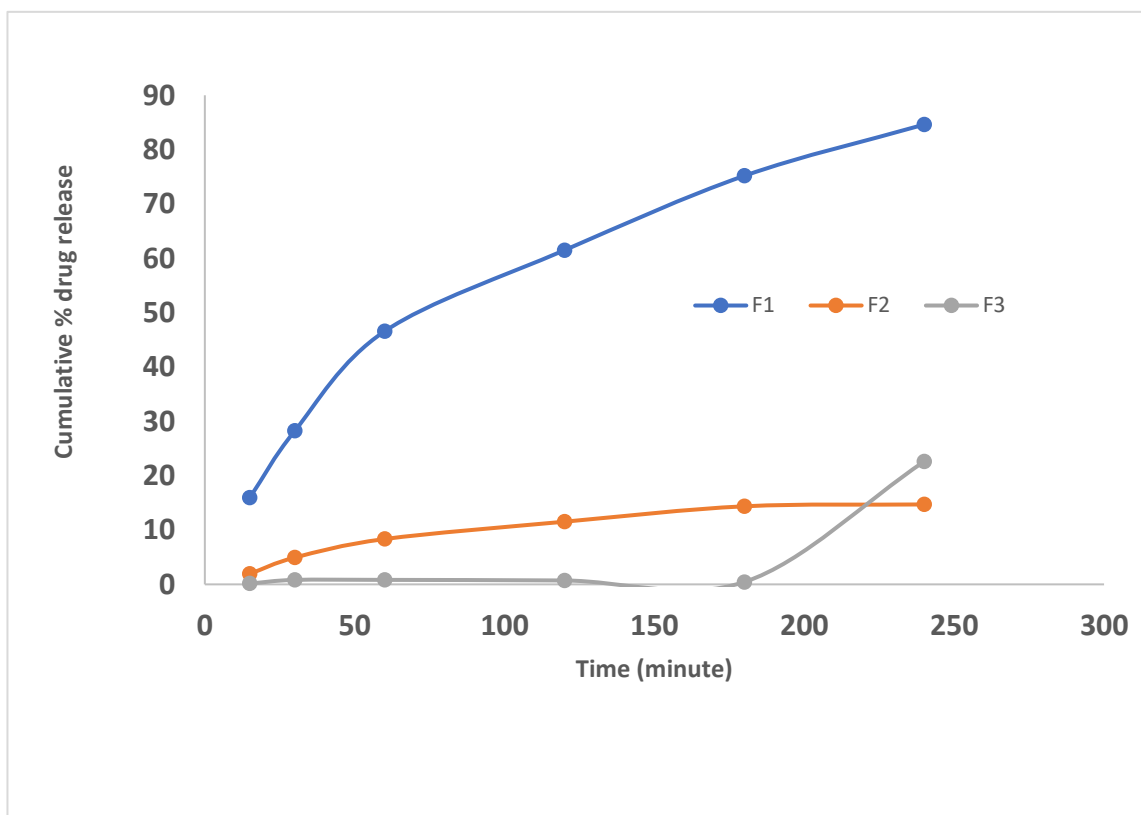
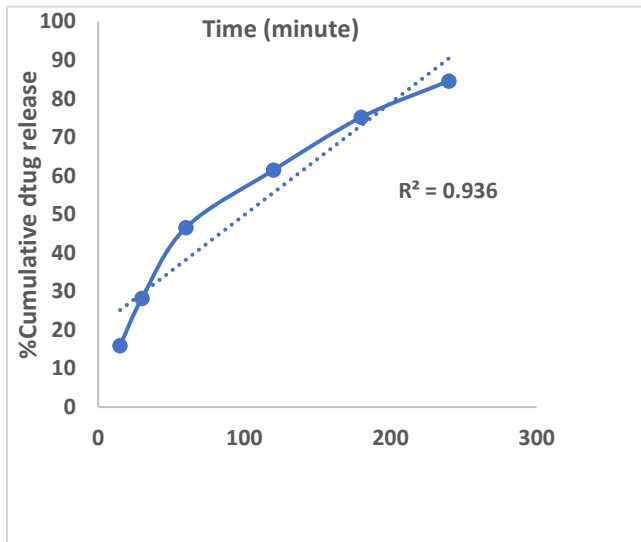
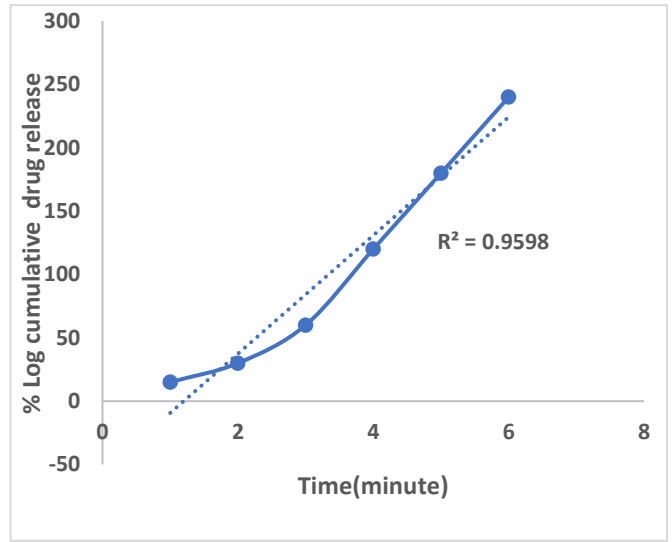


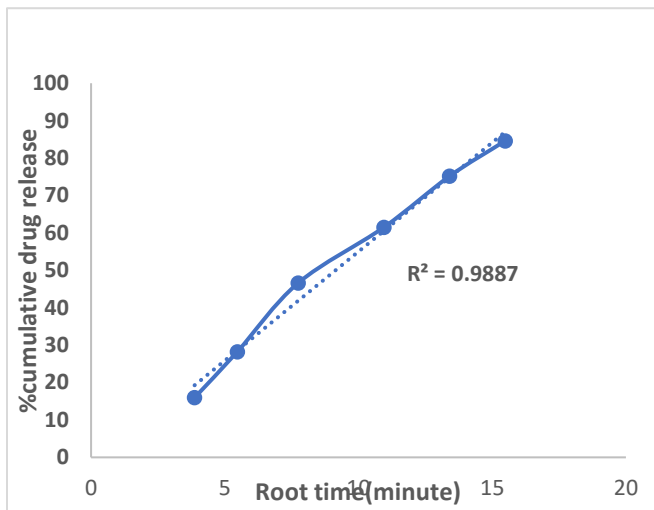
FIG. 7: IN VITRO DRUG RELEASE OF F1, F2, F3



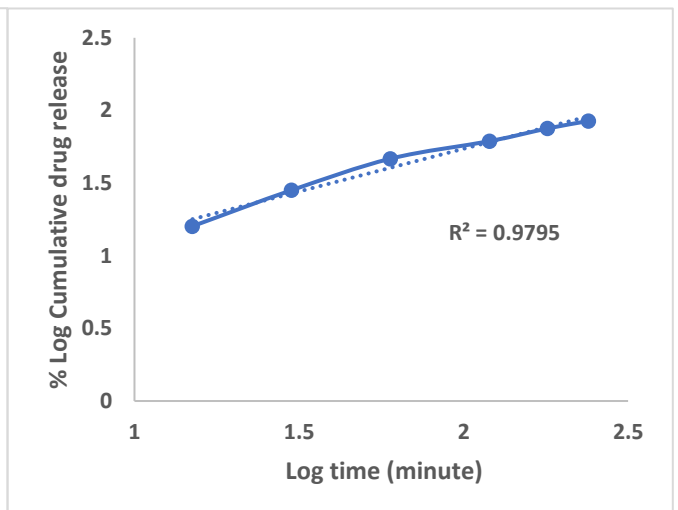
(a)



(b)



(c)



(d)

FIG. 8: (a) ZERO ORDER (b) FIRST ORDER (c) HIGUCHI MODEL (d) KORSEMEYER-PEPPA'S MODEL

### 5.10 Drug entrapment efficiency:

The study shows that entrapment efficiency is affected by the amount and concentration of the polymers, the rate of solvent removal, and some other factors.

The drug entrapment efficiency of the optimized film was lower than the other two formulations, F2 and F3, as those contained a higher amount of pectin. Pectin forms a three-dimensional network that accommodates the drug molecules into it. The entrapment efficiency of the three formulations are given in Table 3.

Formulation code	Pectin: Carbopol	% Entrapment efficiency	(%) Swelling behaviour in pH 7.4 phosphate buffer
F1	1:1	51.34±3.85	98.2
F2	2:1	62.97± 3.04	102.97
F3	3:1	67.9 ± 2.36	135.13

TABLE 3: ENTRAPMENT EFFICIENCY AND SWELLING BEHAVIOUR OF FILMS

Note: (Mean ± SD,  $n = 3$ )

### 5.11 FT-IR Analysis:

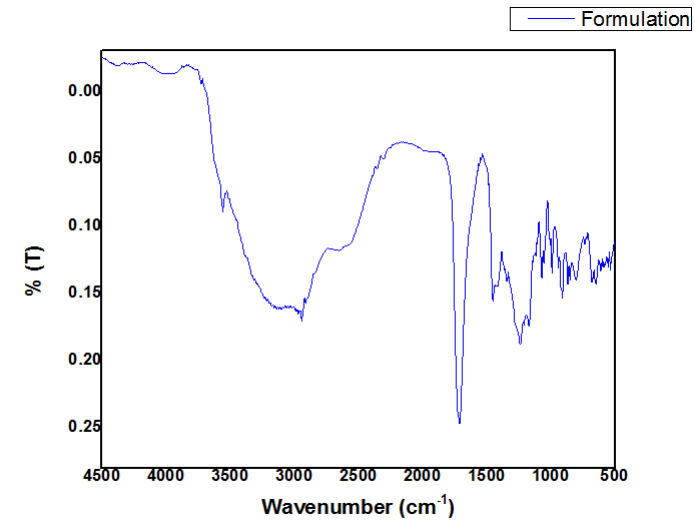
FT-IR of Metformin (Fig.9d) showed three sharp peaks between  $3000\text{ cm}^{-1}$  to  $3500\text{ cm}^{-1}$  which were because of the stretching of NH of the  $\text{NH}_2$  group and CH stretching. Another two peaks were observed near  $1500\text{ cm}^{-1}$  to  $1600\text{ cm}^{-1}$ , and their presence is due to C=N and C-N stretching. For C-H deformation, one peak was also found between  $900$  to  $1000\text{ cm}^{-1}$ .

In the case of Pectin (Fig. 9c), the characteristic band was found between  $3500\text{ cm}^{-1}$  and  $3700\text{ cm}^{-1}$  for O-H stretching, while the peak near  $2900\text{ cm}^{-1}$  was assigned to C-H stretching and another two peaks present within  $1600\text{ cm}^{-1}$  to  $1800\text{ cm}^{-1}$  probably arose from the stretching of asymmetric

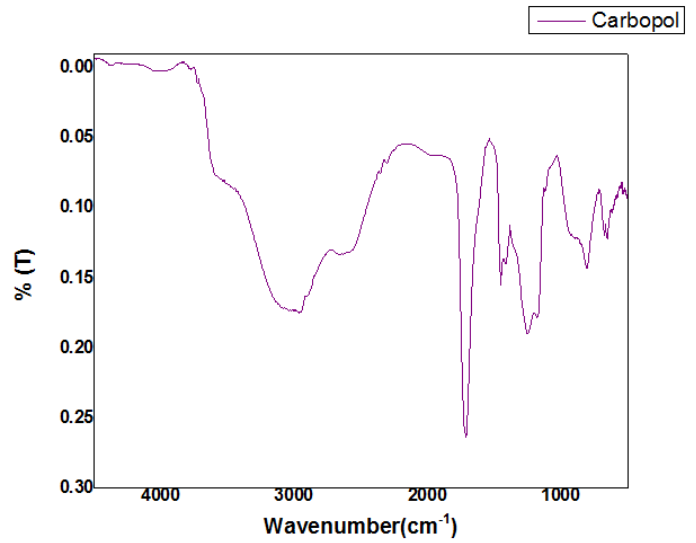
COO- and C=O stretching vibrations of COOH and COOCH<sub>3</sub> groups. The intense band was found at 1014 cm<sup>-1</sup> for the glycosidic bonds connecting two galacturonic sugar units (98).

In the case of C934 (Fig. 9b), -OH stretching vibration and intramolecular hydrogen bonding resulted in the FTIR spectra having a peak between 3000-2950 cm<sup>-1</sup>. The prominent peak between 1750 and 1700 cm<sup>-1</sup> was assigned to carbonyl C=O stretching band. The band at 1275 to 1200 cm<sup>-1</sup> was ascribed to -O-C of acrylates, whereas the peak at 1450 to 1400 cm<sup>-1</sup> was assigned to bending of OH. The C=CH out-of-plane bending band was between 850 and 800 cm<sup>-1</sup> (89). It was evident that Metformin was included in the formulation (Fig. 9a) since it displayed similar peaks of Metformin at 937, 801, and 737 cm<sup>-1</sup>, which are characteristic for -NH wagging. Furthermore, the diminished strength of the Metformin peaks suggests the possibility of the formation of a hydrogen bond with the polymer (99), and the enhanced physical stability of Metformin in the loaded hydrogel was validated by reduced crystallinity, proving that it is present in amorphous form. It also proves the presence of pectin, as a similar peak is present between 3500 to 3700 cm<sup>-1</sup> because of the hydroxyl group. Another band within 2900 to 3000 cm<sup>-1</sup> shows the interaction between Carbopol and Pectin, assigned to the CH stretching. The prominent peak between 1700 and 1750 cm<sup>-1</sup> shows the presence of Carbopol.

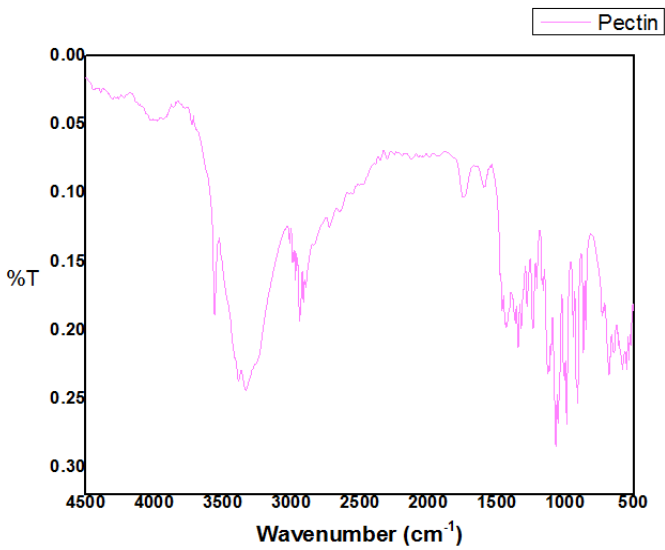




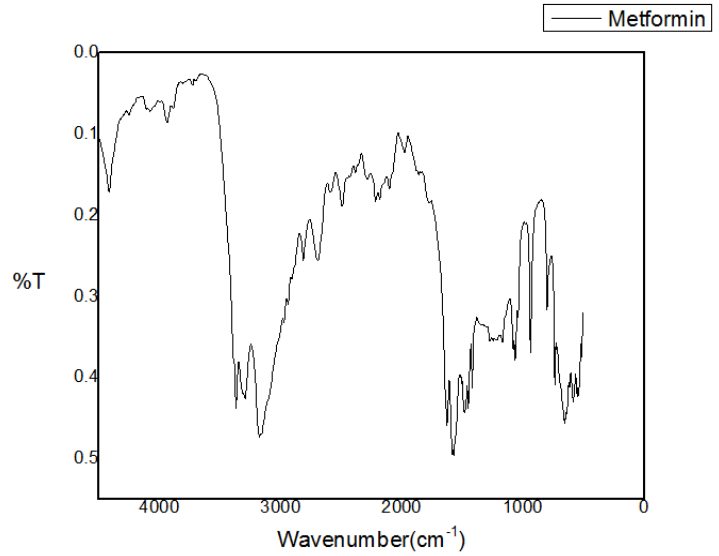
(a)



(b)



(c)



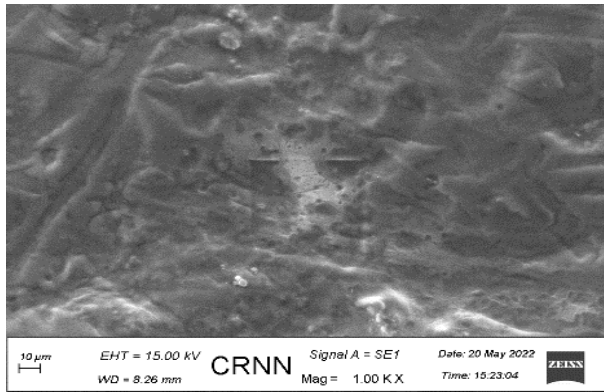
(d)

FIG. 9: FTIR IMAGES (a) FORMULATION (b) CARBOPOL (c) PECTIN (d) METFORMIN

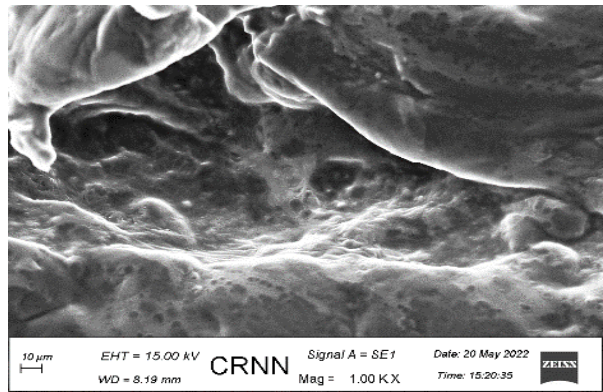
### 5.12 SEM analysis:

Figure 10a represents the rough structure of the Pectin-Carbopol film, which indicates the efficiency of absorbing main substances. Figure 10b represents the void structures of the Pectin – Carbopol film which has the pores within which the drug can be incorporated (100).

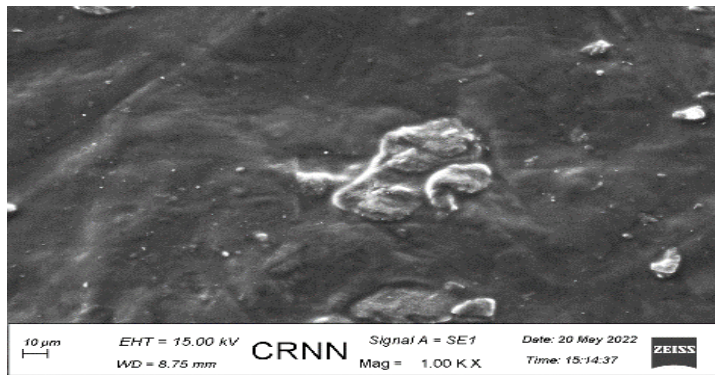
While Fig. 10c shows the micrograph of Pectin- Carbopol film containing the drug Metformin . It can be seen from the micrograph (Fig. 3) that the addition of the drug particles has provided a smoother surface to the film, which further indicates that the drug particles have been successfully embedded in the matrix of the film (98).



(a)



(b)



(c)

FIG. 10:SEM IMAGES (a) BLANK FILM WITHOUT DRUG (b) VOID SPACE OF BLANK FILM (c) FILM LOADED WITH DRUG

### 5.13 XRD analysis:

XRD technique was used to determine the crystallographic properties of the formulation and Metformin, the drug used in the formulation. XRD of pure Metformin shows its peaks between  $10^\circ$  to  $20^\circ$ , another two between  $30^\circ$  to  $40^\circ$ , and the sharpest one at  $23^\circ$  (101). Due to their crystalline composition, Metformin showed prominent peaks that were characteristic of it between  $2\theta$  of  $0^\circ$  and  $70^\circ$ . X ray diffractometry of the formulation shows reduced peak intensity of Metformin, which signifies the excellent interaction of the drug with the polymers and its melting which turns to granulated extrudate, further confirming better drug loading because amorphous substances have a higher solubility than crystalline ones as they have more amount of free lattice energy (90). Other sharp peaks show the presence of the polymers Pectin and Carbopol and their interaction with the drug (98).

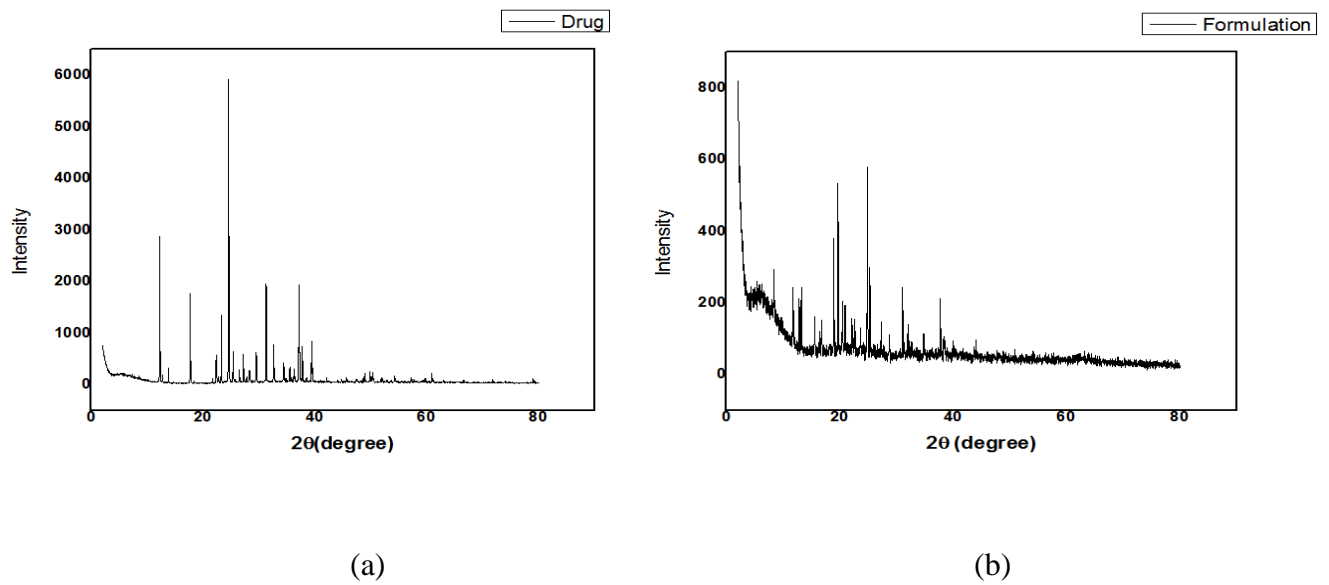


FIG. 11: XRD IMAGES (a) METFORMIN (b) FORMULATION

### 5.14 DSC studies:

Thermal curve of pure Metformin exhibited an initial flat profile followed by a sharp endothermic effect, with a  $T_{\text{peak}}$  at 231.0°C indicating its anhydrous crystalline state. The Differential Scanning Calorimetry study of the formulation shows the presence of Carbopol at the peak between 75 to 100°C and Pectin between 210 to 250°C. Whereas the sharp endothermic peak of Metformin has appeared with a reduced intensity indicating its interaction with the polymers Pectin and Carbopol (102).

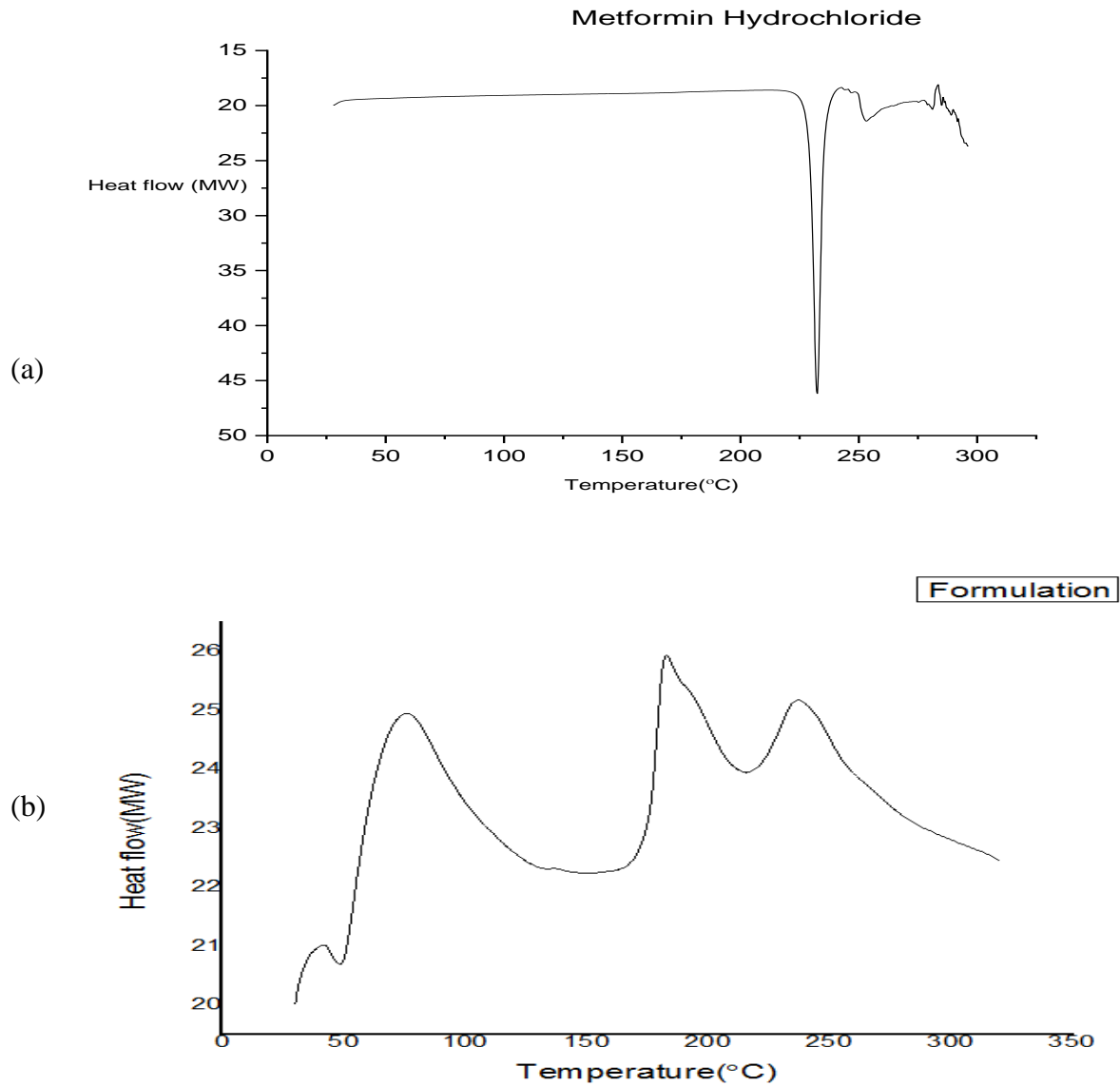


FIG. 12: DSC THERMOGRAM a. METFORMIN HCL b. FORMULATION

### 5.15 Animal studies:

It was shown by the morphological observation that on the second day of creating the wound, there was the presence of erythema and inflammation, indicating a deep second-degree burn wound. After 2 days of creating burn injury the photographs were taken, as the thickness of the wound can be determined after that specific time only in case of burn. This redness increased gradually with time, and the wound started to appear deeper. On the fourth day, the wound of the disease group (group 2) remained almost the same size, while the other two groups (group 3, 4) appeared to be smaller. From the sixth day onwards, the state of the wounds can be differentiated, and there was an effective wound closure rate for the optimized formulation (Group 3), whereas, for the fourth group in which the marketed drug Silver nitrate gel was applied (group 4), appeared to be dry and reduction of wound size was also observed. Moreover, the appearance of the eschar in group 3 confirms the early wound healing procedure (55).

On 8<sup>th</sup> day, abnormal deposition of scar tissue was observed in the Disease group (group 2) which appears like pseudoeschar. The second group, which applied the marketed drug, showed an abnormal contraction, where wound contraction occurred from only one side. Group 3 showed a contraction of the wound with dried eschar. On the twelfth day, eschar fell off naturally, showing a positive sign of wound healing, and the wound size was reduced almost to a dot. Whereas group 4 showed signs of healing, but the rate was delayed and the size of the wound compared to group 3 was more prominent, and group 2 showed a significantly delayed process of wound healing, and the formation of pseudo eschar covered the chronic wound. The morphological studies of the consecutive days are shown below, along with a chart for better understanding.



FIG. 13: Pseudo eschar with deep wound

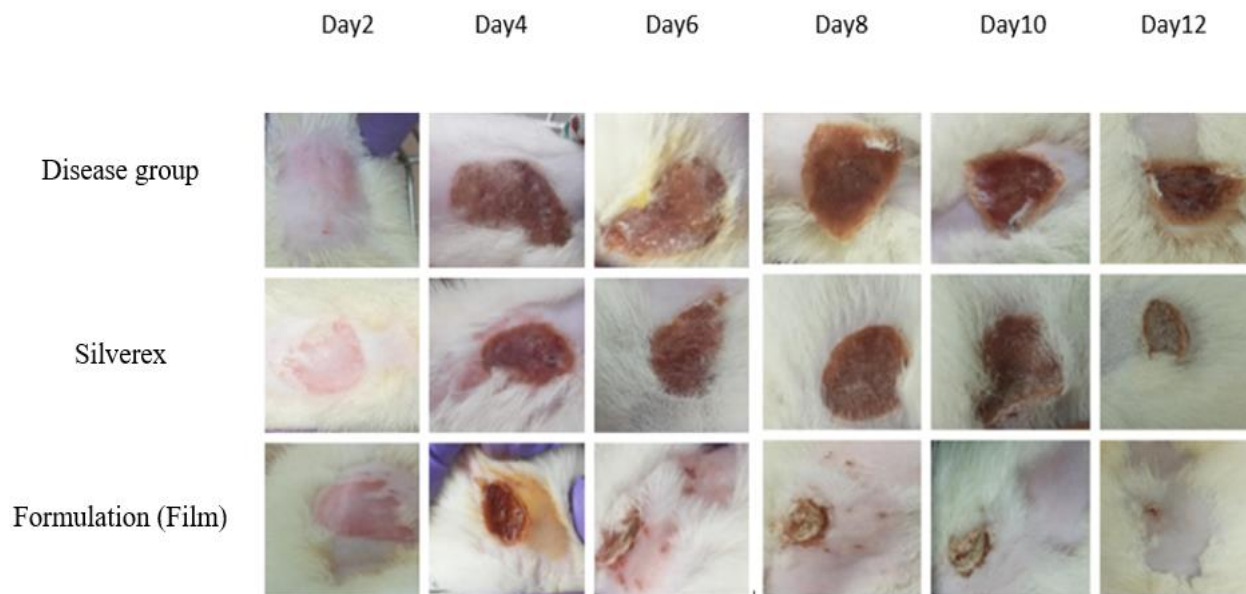


FIG. 14: Morphological studies of wound contraction rate

### 5.15.1 Wound contraction rate:

The wound contraction rate was observed to be highest in the optimized formulation (group 3) group, which was  $98 \pm 2\%$ . In contrast, the untreated control group showed a minimal contraction rate of  $5.2 \pm 3\%$ . The group of animals treated with the marketed silver nitrate gel (group 4) showed better results than the disease group, but it was much lesser than the group who were given the formulated drug. Group 4 showed a result of  $59.47 \pm 5\%$ . The results were plotted in a chart for comparison.

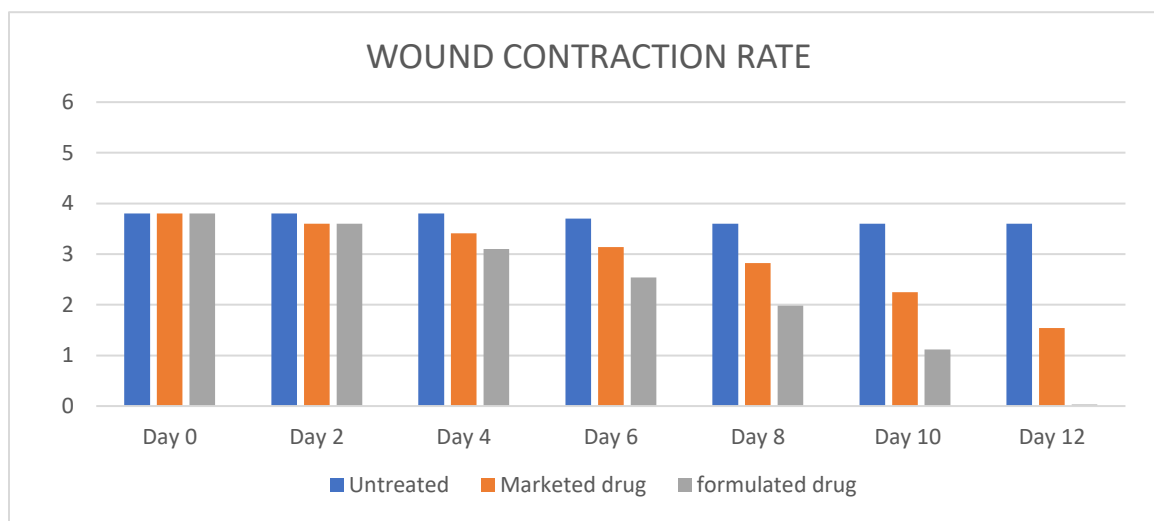


CHART 1: WOUND CONTRACTION RATE

# DISCUSSION

## 6.1 DISCUSSION:

In this experiment, three types of films were developed with varying concentrations of pectin because the other polymer carbopol, when dissolved into water, showed increased viscosity with an increased amount of carbopol. So, the amount of Carbopol has to be constrained in this experiment because otherwise, to limit that disadvantage, more added water made the slurry very diluted, and as a result, the solvent evaporation technique did not work well. Preparing films from that slurry took almost seven to ten days for evaporation of the solvent, and after that, the films' tensile strength was very low, and they could not be peeled off from the Petri dishes. The increasing amount of PEG 400 led to the thickening of the slurry and formation of lumps, which were difficult to homogenize, and from this, it was quite problematic to be poured into Petri dishes to resolve the problem again the water was added as the solvent and that led to the same kind of problem like Carbopol. After adding water, it was again stirred with greater rpm and poured into Petri dishes following the solvent evaporation method. The drying process here also took almost five to seven days, and after drying, the tensile strength was weak, and it tore when peeled it off. Moreover, there were small lumps that were not dissolved properly, and the probable reason for this was more crosslinker, which led to this excessive bonding and forming of lumps. The amount of glycerol was kept limited due to the moist approach. This is because, though the moist approach is good for treating burn wounds, an excessive amount of moisture leads to the development of secondary infection, allowing more bacteria to grow there. So, the amount of pectin was varied in three formulations, and they were named F1, F2, and F3, where the ratio of Pectin and Carbopol was respectively 1:1, 2:1, and 3:1. Results showed that increasing amounts of pectin, improves the tensile strength and along with this, the films were easy to peel off from the Petri dishes. However, there were other problems associated with this. The film's adherence kept decreasing with more pectin added to the film. Following the solvent casting method, the slurries were poured into the Petri dishes, and they took variable but considerable time for evaporation of the solvent; F1 took 24 hours while F2 took nearly 38 hours, and F3 required 52 hours for proper evaporation of the solvent. For this similar reason, the percentage of moisture loss was also found to be minimum in the case of F3, while F1 has optimized moisture loss and F2 has an intermediate value between F1 and F3, but the percentage was not very high. By doing the transparency test, it was visible that F3 was more transparent than F2 and F1 was less transparent than F2 ( $F3 > F2 > F1$ ). It is worth noting that thickness and transparency do not always have to be inversely related. Because when the



identical quantity of solution with various concentrations was placed in a petri dish with a certain diameter, the film thickness relied on the concentration of the solution. However, the microstructure, constituents, and content of polymer films have a greater impact on transparency compared to the thickness. For instance, the film's ingredients' characteristics, the solution's concentration, the degree of homogenization, and the drying conditions often impact the film's microstructure. The increasing amount of pectin increased the transparency and tensile strength of the films but decreased the adherence property of the films, which was not desired. Normal wound dressings tend to get attached to the wound fluid, and difficult to change the dressing due to drying out, which causes severe pain to the patient. This was a reason to develop such films, which would be easy to remove and would not get stuck with the wound fluid, simultaneously providing a moist effect to the wound. Research shows that the moist approach is more efficient in treating burn wounds rather than the dry approach. The important thing that has to be considered for a moist approach is to provide the optimal moist environment. Otherwise, it leads to secondary infection, causing further bacterial growth. So, along with moisture content, the water vapor permeability rate of the films are necessary to assess to prevent such secondary infection in the wound. Depending on the elements like the number of polar groups (hydroxyl groups) on the polymer network's surface, film thickness, and film microstructure, the film's water vapor permeability rate changes. The degree of esterification (DE) of pectin determines the quantity of hydrophilic/polar groups. WVTR reduces with high levels of esterification because there are more hydrophobic ester groups. This justification explains the reason for using chemical-grade pectin in an experiment to obtain comparatively high WVTR. Nevertheless, here another problem evolves. More pectin used in formulation led to decreased water vapor permeability rate for this reason only. Water adsorption and subsequent migration via polar hydroxyl groups often enhance the transportation of water molecules in polymer films. The microstructure of the F3 films would be more compact than the F2 films and similarly to the F1 films when they are formed from the same quantity of material in the same-sized petri dish. This might be what caused WVTR to drop for F3 films as compared to F2 films, providing F1 as the best choice showing the best WVTR. The addition of glycerol did not appear to increase the film's thickness or transparency compared to the same solution concentration. Experiments showed that formulation F1 had the highest WVTR among the three formulations, and it was quite similar to the WVTR of the skin. However, the WVTR rose by 30–40% with the addition of glycerol, which is not the desired outcome. The hygroscopic property of

glycerol is the probable cause of the rise in WVTR. Therefore, while glycerol is a suitable plasticizer to provide the pectin film with high tensile characteristics and flexibility, it also enhances the pectin-carbopol film's hydrophilicity, which raises the WVTR. This rise in Water vapor permeability rate leads to drying out of the wound, which was not expected in the case of a moist approach. By doing the swelling study in the simulated wound fluid model, it was observed that the swelling index was quite higher for F3, and the test of the absorption rate also confirms that. Here also, the formulations followed the same order ( $F3 > F2 > F1$ ), showing the slow rate of absorption of wound fluid in F2 and much slower in F1. It was clearly understood that adding pectin attracted more water molecules at a faster rate, leading to quick absorption of wound fluid and a higher swelling index. Nevertheless, in vitro release studies confirm that adding pectin, though it provides positive results for absorption rate and swelling index, did not show any promising results in releasing the drug. F3 showed an anomalous drug release at the end of four hours, while there was minimal release throughout the study. F2 released only  $22.61 \pm 7.12\%$  of the drug throughout the study, and there was no sudden drug release at the end. Whereas F1 provides a very positive result and shows a constant rate of release, following the Higuchi model, the release at the end of four hours was about 87%. The probable reason for this kind of result was the higher range of swelling index and a higher rate of absorption in the case of F2 and F3. The release from the polymeric matrix was due to the relaxation of the polymeric network by the slow entrance of the solvent molecules within it, which was only satisfied by F1, where solvent entered at a controlled rate and, in this way, provided a precise loosening of polymeric network and regulated the drug release. The Higuchi model further confirms the presence of very small Metformin Hydrochloride particles embedded in a thick polymeric matrix composed of Pectin and Carbopol, and drug diffusivity was constant. Films of the F2 model showed quicker solvent absorption, but that was not enough to loosen all the polymeric chains and release the drug in a controlled manner. At the end of four hours, the drug was not released properly for this reason. F3 formulations show the quickest absorption of the solvent molecules, and because of the presence of more pectin molecules, films attracted a huge quantity of solvent, which penetrated the films and lastly resulted in a sudden burst of the release of the drug molecules at the end of four hours. All three formulations were perfectly soluble in water. They took variable time to dissolve, but that difference was negligible. F1 films quickly dissolved in water, while F2 and F3 took a little more time, and this was probably due to the presence of the higher amount of pectin in the water.

Increasing or decreasing the amount of flaxseed extract did not affect the formulation or the results. Only the transparency of the films decreased when the excessive quantity of flaxseed mucilage was added, and this was probably due to the presence of protein. Most researchers took only the flaxseed gel, but in this experiment, the gel, along with the protein, was used to enhance the restoration of the skin structure. The use of flaxseed protein along with the mucilage enhanced the moisturization purpose of the film along with enhancing the wound healing process. The surface morphology of the optimized film F1 came as smooth, which signifies the presence of Metformin particles embedded in the matrix, as the SEM micrographs of the films without drug loading appeared rough. The XRD and FTIR analysis confirms the presence and interaction of the drug Metformin Hydrochloride with the other polymers, as the peak of reduced intensity, signifies it. The entrapment efficiency of the optimized formulation was lesser than the other two formulations, F2 and F3. As the amount of pectin increased in the formulation, enhanced entrapment efficiency was observed. However, this also showed less release of drugs from F2 and F3. Those films entrapped the drug in a good manner, but the release was not constant as it was so embedded in the polymeric matrix. Moreover, in the in-vivo models, there were four groups of Wistar rats weighing  $150 \pm 20$  g. The first group consisted of healthy rats considered as control, while the second group was taken as the Disease group (group 2), and they were left untreated to observe the rate of wound healing without any treatment. While one of the other two groups was treated with the marketed drug (group 4), another group of rats was treated with the formulated film (group 3) to compare the progress of rate of wound healing. Rats of the three groups (2,3,4) were resuscitated immediately with the ringer's lactate solution (intraperitoneal route injection) after the creation of the burn wound. The marketed drug and films were given to the rats for 12 days and were treated once daily. At the end of the experiment, the Disease group (group 2) showed the least rate of wound contraction along with the formation of thick pseudo eschar. There was the presence of a wound in the active form underneath the pseudo eschar. That presence of pseudo eschar indicated the abnormal deposition of the scar tissue. A Group of the animals who applied silver nitrate gel, the go-to option for burn wounds in the market, showed a contraction of the wound from one side, which should be from both ends, and that indicated abnormality on the tenth day. However, on the twelfth day, the wound contraction rate was much higher than the Disease group, but there was no formation of eschar or deposition of granulation tissue which signifies that it had not entered the phase of wound remodeling stage. Whereas the group who were given the optimized formulation

once daily showed a consistent rate of wound contraction along with the formation of eschar on the sixth day only. Day by day, the eschar was dried, and both ends of the wound came closer quickly. The eschar fell off naturally on the twelfth day only without any active wound or bleeding. The formation of eschar indicated a very positive sign in wound healing as it signified that the healing process was accelerated, and after the formation of the granulation tissue, the wound entered the fourth healing stage, remodeling. It further proved that the moist approach and covering the wound with film worked well compared to group M where the wounds were left open after applying the silver nitrate gel. The films automatically adhere to the skin, which was very easy to remove the next day. A big breakthrough in treating people with type 2 diabetes, metformin is a synthetic guanidine derivative derived from *Galega officinalis* extracts (106). Emerging data recently showed that metformin reduced the production of pro-inflammatory cytokines, shielded cells from oxidative damage, and polarised macrophages both in vitro and in vivo (107,108 ,109). Zhao and his coworker (107) found that metformin administered locally sped up wound healing in young rats and enhanced their epidermis, hair follicles, and collagen deposition. Despite the prior research describing metformin's capacity to reduce inflammation and direct macrophages, it is still unclear how these factors interact with wound healing, macrophage polarisation, the NLRP3 inflammasome, and metformin. Qing et al. examined the therapeutic impact of metformin on wound healing in the study and looked into its underlying mechanisms. Those findings unambiguously showed that metformin therapy is a successful therapeutic approach for enhancing wound healing by preventing NLRP3 inflammasome activation to control macrophage polarisation. These findings all pointed to the fact that metformin offers novel therapeutic potential for the treatment of wound healing. Macrophages are a diverse population of cells that can be activated in one of two ways—classical M1 or alternative M2—in response to different inputs. Previous research has shown that M1 macrophage polarisation is crucial for the initial phases of wound healing and that it increases and sustains the inflammatory response by releasing significant amounts of pro-inflammatory cytokines and ROS (1-3). It has been suggested that M2 macrophage polarisation is connected to the process of tissue healing activities. There is increasing evidence that M2 macrophages control collagen formation, regeneration of fibroblasts, myofibroblast differentiation, and re-vascularization during the healing of wounds (110,111). The proliferative stage of repair in diabetic wounds is regulated by growth factors like TGF-, insulin-like growth factor-1 (IGF-1), and vascular endothelial growth factor (VEGF), according to previous studies

(112-114). Reduced M2 macrophage levels also result in reduced levels of these growth factors. Additionally, the non-healing phenotype was influenced by high amounts of pro-inflammatory cytokines and mediators, including TNF, IL-1, IL-17, and iNOS (115,116). It has been suggested that increasing the amount of M2 macrophages in the wound may hasten wound closure since M2 macrophage cells have been shown to enhance wound healing. Metformin administration enhances alternative M2 macrophage polarisation in vivo and in vitro, as seen in the current study (33). They also studied the molecular mechanism of Metformin Hydrochloride, which shows its inducing effect in M2 macrophage polarization during the wound healing process along with the suppression of the expression of caspase-1, IL-1 $\beta$ , and NLRP3, in vivo and vitro. The NLRP3 inflammasome, a multi-protein complex, along with NLRP3, ASC, and caspase-1, regulates the activity of caspase-1 and the production of the inflammatory cytokines IL-1 and IL-18 by the innate immune system. The wound healing process has been discovered to entail inflammasome signaling and downstream cytokine responses, which are mediated by the inflammasome (117). Recent research suggests that inhibiting the NLRP3 inflammasome is one of the main factors speeding up the healing of wounds in diabetic mice (118). Previous research had suggested that NLRP3 inflammasome activation may be a factor in the slow healing of wounds in diabetes patients. On the other hand, when NLRP3 inflammasome was negatively regulated, it suggested a possible therapeutic target for enhancing wound healing. Importantly, topical administration of pharmacological inhibitors to mice's wounds accelerated healing, triggered a transition from pro-inflammatory (M1 macrophage) to healing-associated macrophage (M2 macrophage) phenotypes, and elevated pro-healing growth factors (119). Recent research has shown that metformin primarily reduces immunological responses by directly affecting the cellular processes of different immune cell types by inducing AMPK and subsequently inhibiting mTOR (121,120). Intestinal inflammation is reduced when the mTOR/NLRP3 signaling pathway is inhibited. According to a recent, scientists also identified NLRP3 as mTOR's binding partner (122). As demonstrated in the current work, metformin administration induces the activation of AMPK, which promotes alternative M2 macrophage polarisation. Activation of the mTOR/NLRP3 inflammasome signaling pathway can be inhibited by activating and phosphorylating AMPK. Therefore, Qing and his colleagues concluded that metformin's ability to speed up wound healing might be due to its ability to change macrophage phenotype via modulating the AMPK/mTOR/NLRP3 inflammasome signaling axis(33).

# CONCLUSION

## 7.1 CONCLUSION

In a nutshell, the film F1 was optimized based on the studies like moisture content, water vapor permeability rate, drug entrapment efficiency, *in-vitro* release studies, and more factors described above. Physicochemical characterizations of optimized formulation indicated all requisite properties of moist film for being a potent approach to treating second-degree burn wounds. The animals were treated with this optimized film which showed a positive result. *In-vitro* release studies also confirmed the drug's controlled release to the wound site at a constant rate following the Higuchi model. This study found that Metformin administration enhanced the process of wound healing by suppressing NLRP3 inflammasome activations and macrophage polarisation along with controlling the AMPK/mTOR signaling pathway. This pathway blockade was used to suppress the activation of the NLRP3 inflammasome, which increased M2 macrophage polarisation and sped up wound healing by applying Metformin Hydrochloride topically.

# REFERENCES



## 8.1 REFERENCES:

1. Lim KM. Skin epidermis and barrier function. *International Journal of Molecular Sciences*. 2021 Mar 16;22(6):3035.
2. Bucknall TE. Factors affecting wound-healing. *Problems in General Surgery*. 1989 Apr 1;6(2):194-219.
3. Viollet B, Guigas B, Garcia N, Leclerc J, Foretz M, Andreelli F. Mecanismos celulares y moleculares de metformina: Una vision general. *Clin. Sci. (Lond)*. 2012; 6:253-70.
4. EA RM, Burmeister DM, Rose LF, Natesan S, Chan RK, Christy RJ, Chung KK. *Crit. Care*. 2015; 19:243.
5. Official website of World Health Organization
6. Arturson G. Pathophysiology of the burn wound. In *Annales chirurgiae et gynaecologiae* 1980 Jan 1 (Vol. 69, No. 5, pp. 178-190).
7. Mathieu D, Wattel F. Physiologic effects of hyperbaric oxygen on microorganisms and host defences against infection. In *Handbook on Hyperbaric Medicine 2006* (pp. 103-119). Springer, Dordrecht.
8. Woo K, Ayello EA, Sibbald RG. The edge effect: current therapeutic options to advance the wound edge. *Advances in skin & wound care*. 2007 Feb 1;20(2):99-117.
9. Vincent AM, Russell JW, Low P, Feldman EL. Oxidative stress in the pathogenesis of diabetic neuropathy. *Endocrine reviews*. 2004 Aug 1;25(4):612-28.
10. Hong WX, Hu MS, Esquivel M, Liang GY, Rennert RC, McArdle A, Paik KJ, Duscher D, Gurtner GC, Lorenz HP, Longaker MT. The role of hypoxia-inducible factor in wound healing. *Advances in wound care*. 2014 May 1;3(5):390-9.
11. Liodaki E, Senyaman Ö, Stollwerck PL, Möllmeier D, Mauss KL, Mailänder P, Stang F. Obese patients in a burn care unit: a major challenge. *Burns*. 2014 Dec 1;40(8):1738-42.
12. Evers LH, Bhavsar D, Mailänder P. The biology of burn injury. *Experimental dermatology*. 2010 Sep;19(9):777-83.
13. Kolarsick PA, Kolarsick MA, Goodwin C. Anatomy and physiology of the skin. *Journal of the Dermatology Nurses' Association*. 2011 Jul 1;3(4):203-13.
14. Abdel-Sayed P, Michetti M, Scaletta C, Flahaut M, Hirt-Burri N, de Buys Roessingh A, Raffoul W, Applegate LA. Cell therapies for skin regeneration: an overview of 40 years of experience in burn units. *Swiss medical weekly*. 2019 May 19;149(1920). Nisanci M,

- Eski M, Sahin I, Ilgan S, Isik S. Saving the zone of stasis in burns with activated protein C: an experimental study in rats. *Burns*. 2010 May 1;36(3):397-402.
15. Strudwick XL, Cowin AJ. The role of the inflammatory response in burn injury. *Hot topics in burn injuries*. 2018 May 23:38-61.
  16. Gravante G, Filingeri V, Delogu D, Santeusano G, Palmieri MB, Esposito G, Montone A, Sconocchia G. Apoptotic cell death in deep partial thickness burns by coexpression analysis of TUNEL and Fas. *Surgery*. 2006 Jun 1;139(6):854-5.
  17. Singer AJ, Thode Jr HC, McClain SA. Development of a histomorphologic scale to quantify cutaneous scars after burns. *Academic Emergency Medicine*. 2000 Oct;7(10):1083-8.
  18. Clark RA. Wound repair. Overview and general considerations. *The molecular and cellular biology of wound repair*. 1994.
  19. Szpaderska AM, Egozi EI, Gamelli RL, DiPietro LA. The effect of thrombocytopenia on dermal wound healing. *Journal of Investigative Dermatology*. 2003 Jun 1;120(6):1130-7.
  20. Malaviya R, Ikeda T, Ross E, Abraham SN. Mast cell modulation of neutrophil influx and bacterial clearance at sites of infection through TNF- $\alpha$ . *Nature*. 1996 May;381(6577):77-80.
  21. Lou O, Alcaide P, Luscinskas FW, Muller WA. CD99 is a key mediator of the transendothelial migration of neutrophils. *The Journal of Immunology*. 2007 Jan 15;178(2):1136-43.
  22. Lian Z, Yin X, Li H, Jia L, He X, Yan Y, Liu N, Wan K, Li X, Lin S. Synergistic effect of bone marrow-derived mesenchymal stem cells and platelet-rich plasma in streptozotocin-induced diabetic rats. *Annals of dermatology*. 2014 Feb 1;26(1):1-0.
  23. Weller K, Foitzik K, Paus R, Syska W, Maurer M, Weller K, Foitzik K, Paus R, Syska W, Maurer M. Mast cells are required for normal healing of skin wounds in mice. *The FASEB journal*. 2006 Nov;20(13):2366-8.
  24. Maurer M, Theoharides T, Granstein RD, Bischoff SC, Bienenstock J, Henz B, Kovanen P, Piliponsky AM, Kambe N, Vliagoftis H, Levi-Schaffer F. What is the physiological function of mast cells? *Experimental dermatology*. 2003 Dec;12(6):886-.
  25. Weber A, Knop J, Maurer M. Pattern analysis of human cutaneous mast cell populations by total body surface mapping. *British Journal of Dermatology*. 2003 Feb;148(2):224-8.

26. Galli SJ. New concepts about the mast cell. *New England Journal of Medicine*. 1993 Jan 28;328(4):257-65.
27. Singer AJ, Thode Jr HC, McClain SA. Development of a histomorphologic scale to quantify cutaneous scars after burns. *Academic Emergency Medicine*. 2000 Oct;7(10):1083-8.
28. Stewart KJ. A quantitative ultrastructural study of collagen fibrils in human skin normal scars, and hypertrophic scars. *Clinical Anatomy: The Official Journal of the American Association of Clinical Anatomists and the British Association of Clinical Anatomists*. 1995;8(5):334-8.
29. Opalenik SR, Davidson JM. Fibroblast differentiation of bone marrow-derived cells during wound repair. *The FASEB Journal*. 2005 Sep;19(11):1561-3.
30. Montesano R, Orci L. Transforming growth factor beta stimulates collagen-matrix contraction by fibroblasts: implications for wound healing. *Proceedings of the National Academy of Sciences*. 1988 Jul;85(13):4894-7.
31. Gurtner GC, Werner S, Barrandon Y, Longaker MT. Wound repair and regeneration. *Nature*. 2008 May;453(7193):314-21.
32. Qing L, Fu J, Wu P, Zhou Z, Yu F, Tang J. Metformin induces the M2 macrophage polarization to accelerate the wound healing via regulating AMPK/mTOR/NLRP3 inflammasome signaling pathway. *Am J Transl Res*. 2019 Feb 15;11(2):655-668. PMID: 30899369; PMCID: PMC6413292.
33. Bitto A, Altavilla D, Pizzino G, Irrera N, Pallio G, Colonna MR, Squadrito F. Inhibition of inflammasome activation improves the impaired pattern of healing in genetically diabetic mice. *British journal of pharmacology*. 2014 May;171(9):2300-7.
34. Cavalcante-Silva J, Koh TJ. Targeting the NOD-Like Receptor Pyrin Domain Containing 3 Inflammasome to Improve Healing of Diabetic Wounds. *Advances in Wound Care*. 2022 Jan 13.
35. Zhang BC, Li Z, Xu W, Xiang CH, Ma YF. Luteolin alleviates NLRP3 inflammasome activation and directs macrophage polarization in lipopolysaccharide-stimulated RAW264. 7 cells. *American Journal of Translational Research*. 2018;10(1):265.

36. Cunha C, Gomes C, Vaz AR, Brites D. Exploring new inflammatory biomarkers and pathways during LPS-induced M1 polarization. *Mediators of Inflammation*. 2016 Oct;2016.
37. Aitcheson SM, Frentiu FD, Hurn SE, Edwards K, Murray RZ. Skin wound healing: normal macrophage function and macrophage dysfunction in diabetic wounds. *Molecules*. 2021 Aug 13;26(16):4917.
38. Hesketh M, Sahin KB, West ZE, Murray RZ. Macrophage phenotypes regulate scar formation and chronic wound healing. *International journal of molecular sciences*. 2017 Jul 17;18(7):1545.
39. Krzyszczyk P, Schloss R, Palmer A, Berthiaume F. The role of macrophages in acute and chronic wound healing and interventions to promote pro-wound healing phenotypes. *Frontiers in physiology*. 2018 May 1;9:419.
40. Anders HJ, Suarez-Alvarez B, Grigorescu M, Foresto-Neto O, Steiger S, Desai J, Marschner JA, Honarpisheh M, Shi C, Jordan J, Müller L. The macrophage phenotype and inflammasome component NLRP3 contributes to nephrocalcinosis-related chronic kidney disease independent from IL-1-mediated tissue injury. *Kidney international*. 2018 Mar 1;93(3):656-69.
41. Koese O, Waseem A. Keloids and hypertrophic scars: are they two different sides of the same coin?. *Dermatologic surgery*. 2008 Mar;34(3):336-46.
42. Wu M, Xu H, Liu J, Tan X, Wan S, Guo M, Long Y, Xu Y. Metformin and fibrosis: a review of existing evidence and mechanisms. *Journal of Diabetes Research*. 2021 Apr 29;2021.
43. Meng S, Cao J, He Q, Xiong L, Chang E, Radovick S, Wondisford FE, He L. Metformin activates AMP-activated protein kinase by promoting formation of the  $\alpha\beta\gamma$  heterotrimeric complex. *Journal of Biological Chemistry*. 2015 Feb 6;290(6):3793-802.
44. Kotwal GJ, Chien S. Macrophage differentiation in normal and accelerated wound healing. *Macrophages*. 2017:353-64.
45. Ito H, Kanbe A, Sakai H, Seishima M. Activation of NLRP 3 signalling accelerates skin wound healing. *Experimental dermatology*. 2018 Jan;27(1):80-6.
46. Markov PA, Khramova DS, Shumikhin KV, Nikitina IR, Beloseroov VS, Martinson EA, Litvinets SG, Popov SV. Mechanical properties of the pectin hydrogels and inflammation

- response to their subcutaneous implantation. *Journal of Biomedical Materials Research Part A*. 2019 Sep;107(9):2088-98.
47. Shahzad A, Khan A, Afzal Z, Umer MF, Khan J, Khan GM. Formulation development and characterization of cefazolin nanoparticles-loaded cross-linked films of sodium alginate and pectin as wound dressings. *International journal of biological macromolecules*. 2019 Mar 1;124:255-69.
48. Kaşgöz H, Aydın İ, Kaşgöz A. The effect of PEG (400) DA crosslinking agent on swelling behaviour of acrylamide-maleic acid hydrogels. *Polymer bulletin*. 2005 Jul;54(6):387-97.
49. Winter GD. Formation of the scab and the rate of epithelization of superficial wounds in the skin of the young domestic pig. *Nature*. 1962 Jan;193(4812):293-4.
50. Dyson M, Young SR, Hart J, Lynch JA, Lang S. Comparison of the effects of moist and dry conditions on the process of angiogenesis during dermal repair. *Journal of Investigative Dermatology*. 1992 Dec 1;99(6):729-33.
51. Demling RH, DeSanti L. Effects of silver on wound management. *Wounds*. 2001;13(1):4-15.
52. Monafo WW, West MA. Current treatment recommendations for topical burn therapy. *Drugs*. 1990 Sep;40(3):364-73.
53. Klasen HJ. A historical review of the use of silver in the treatment of burns. II. Renewed interest for silver. *Burns*. 2000 Mar 1;26(2):131-8.
54. Monsuur HN, Van den Broek LJ, Jhingorie RL, Vloemans AF, Gibbs S. Burn eschar stimulates fibroblast and adipose mesenchymal stromal cell proliferation and migration but inhibits endothelial cell sprouting. *International journal of molecular sciences*. 2017 Aug 18;18(8):1790.
55. Jeschke MG, Abdullahi A, Burnett M, Rehou S, Stanojic M. Glucose control in severely burned patients using metformin: an interim safety and efficacy analysis of a phase II randomized controlled trial. *Annals of surgery*. 2016 Sep;264(3):518.
56. Border WA, Ruoslahti E. Transforming growth factor-beta in disease: the dark side of tissue repair. *The Journal of clinical investigation*. 1992 Jul 1;90(1):1-7.
57. Gilani S, Mir S, Masood M, Khan AK, Rashid R, Azhar S, Rasul A, Ashraf MN, Waqas MK, Murtaza G. Triple-component nanocomposite films prepared using a casting

- method: Its potential in drug delivery. *Journal of Food and Drug Analysis*. 2018 Apr 1;26(2):887-902.
58. Beroual K, Agabou A, Abdeldjelil MC, Boutaghane N, Haouam S, Hamdi-Pacha Y. Evaluation of crude flaxseed (*Linum usitatissimum* L.) oil in burn wound healing in New Zealand rabbits. *African Journal of Traditional, Complementary and Alternative Medicines*. 2017 Apr 13;14(3):280-6.
59. Markov PA, Popov SV, Nikitina IR, Ovodova RG, Ovodov YS. Anti-inflammatory activity of pectins and their galacturonan backbone. *Russian Journal of Bioorganic Chemistry*. 2011 Dec;37(7):817-21.
60. Ovodov YS. Current views on pectin substances. *Russian Journal of Bioorganic Chemistry*. 2009 May;35(3):269-84.
61. Birch NP, Barney LE, Pandres E, Peyton SR, Schiffman JD. Thermal-responsive behavior of a cell compatible chitosan/pectin hydrogel. *Biomacromolecules*. 2015 Jun 8;16(6):1837-43.
62. Chen CH, Sheu MT, Chen TF, Wang YC, Hou WC, Liu DZ, Chung TC, Liang YC. Suppression of endotoxin-induced proinflammatory responses by citrus pectin through blocking LPS signaling pathways. *Biochemical Pharmacology*. 2006 Oct 16;72(8):1001-9.
63. Tummalapalli M, Berthet M, Verrier B, Deopura BL, Alam MS, Gupta B. Drug loaded composite oxidized pectin and gelatin networks for accelerated wound healing. *International Journal of Pharmaceutics*. 2016 May 30;505(1-2):234-45.
64. Grip J, Engstad RE, Skjæveland I, Škalko-Basnet N, Holsæter AM. Sprayable Carbopol hydrogel with soluble beta-1, 3/1, 6-glucan as an active ingredient for wound healing—development and in-vivo evaluation. *European Journal of Pharmaceutical Sciences*. 2017 Sep 30;107:24-31.
65. Hayati F, Ghamsari SM, Dehghan MM, Oryan A. Effects of carbomer 940 hydrogel on burn wounds: an in vitro and in vivo study. *Journal of Dermatological Treatment*. 2018 Aug 18;29(6):593-9.
66. Demirci S, Doğan A, Karakuş E, Halıcı Z, Topçu A, Demirci E, Sahin F. Boron and poloxamer (F68 and F127) containing hydrogel formulation for burn wound healing. *Biological Trace Element Research*. 2015 Nov;168(1):169-80.

67. Song Z, Wen Y, Teng F, Wang M, Liu N, Feng R. Carbopol 940 hydrogel containing curcumin-loaded micelles for skin delivery and application in inflammation treatment and wound healing. *New Journal of Chemistry*. 2022;46(8):3674-86.
68. Kim J, Lee CM. Transdermal hydrogel composed of polyacrylic acid containing Propolis for wound healing in a rat model. *Macromolecular Research*. 2018 Dec;26(13):1219-24.
69. Kim BS, Im JS, Baek ST, Lee JO, Sigeta M, Yoshinaga K. Synthesis of polyglycidol hydrogel films crosslinked with carboxyl-terminated poly (ethylene glycol). *Polymer journal*. 2006 Apr;38(4):335-42.
70. Brøndsted H, Andersen C, Hovgaard L. Crosslinked dextran—a new capsule material for colon targeting of drugs. *Journal of controlled Release*. 1998 Apr 30;53(1-3):7-13.
71. Dweck A. Herbal medicine for the skin. Their chemistry and effects on skin and mucous membranes. *Journal of applied cosmetology*. 2002;20(1):83-.
72. Cunnane SC, Hamadeh MJ, Liede AC, Thompson LU, Wolever TM, Jenkins DJ. Nutritional attributes of traditional flaxseed in healthy young adults. *The American Journal of Clinical Nutrition*. 1995 Jan 1;61(1):62-8.
73. McDaniel JC, Belury M, Ahijevych K, Blakely W. Omega-3 fatty acids effect on wound healing. *Wound Repair and Regeneration*. 2008 May;16(3):337-45.
74. Pellizzon MA, Billheimer JT, Bloedon LT, Szapary PO, Rader DJ. Flaxseed reduces plasma cholesterol levels in hypercholesterolemic mouse models. *Journal of the American College of Nutrition*. 2007 Feb 1;26(1):66-75.
75. Loden M, Andersson AC. Effect of topically applied lipids on surfactant-irritated skin. *British Journal of Dermatology*. 1996 Feb;134(2):215-20.
76. Yang J, Wang Z, Wang S. Glycerol-regulated tough and electroresponsive alginate hydrogels for a muscle-like biobased polymer actuator with highly sensitive and durable output force. *Journal of Applied Polymer Science*. 2021 Dec 15;138(47):51393.
77. Fluhr JW, Bornkessel A, Berardesca E. Glycerol—just a moisturizer? Biological and biophysical effects. In *Dry Skin and Moisturizers 2005* Nov 9 (pp. 243-260). CRC Press.
78. Lee JO, Lee SK, Jung JH, Kim JH, You GY, Kim SJ, Park SH, Uhm KO, Kim HS. Metformin induces Rab4 through AMPK and modulates GLUT4 translocation in skeletal muscle cells. *Journal of cellular physiology*. 2011 Apr;226(4):974-81.

79. Lee SK, Lee JO, Kim JH, Kim SJ, You GY, Moon JW, Jung JH, Park SH, Uhm KO, Park JM, Suh PG. Metformin sensitizes insulin signaling through AMPK-mediated pten down-regulation in preadipocyte 3T3-L1 cells. *Journal of cellular biochemistry*. 2011 May;112(5):1259-67.
80. Jalving M, Gietema JA, Lefrandt JD, de Jong S, Reyners AK, Gans RO, de Vries EG. Metformin: taking away the candy for cancer?. *European journal of cancer*. 2010 Sep 1;46(13):2369-80.
81. Min AK, Jeong JY, Go Y, Choi YK, Kim YD, Lee IK, Park KG. cAMP response element binding protein H mediates fenofibrate-induced suppression of hepatic lipogenesis. *Diabetologia*. 2013 Feb;56(2):412-22.
82. Rice S, Pellatt LJ, Bryan SJ, Whitehead SA, Mason HD. Action of metformin on the insulin-signaling pathway and on glucose transport in human granulosa cells. *The Journal of Clinical Endocrinology & Metabolism*. 2011 Mar 1;96(3):E427-35.
83. Oh TJ, Shin JY, Kang GH, Park KS, Cho YM. Effect of the combination of metformin and fenofibrate on glucose homeostasis in diabetic Goto-Kakizaki rats. *Experimental & molecular medicine*. 2013 Jul;45(7):e30-.
84. Turban S, Stretton C, Drouin O, Green CJ, Watson ML, Gray A, Ross F, Lantier L, Viollet B, Hardie DG, Marette A. Defining the contribution of AMP-activated protein kinase (AMPK) and protein kinase C (PKC) in regulation of glucose uptake by metformin in skeletal muscle cells. *Journal of Biological Chemistry*. 2012 Jun 8;287(24):20088-99.
85. Stephenne X, Foretz M, Taleux N, Van Der Zon GC, Sokal E, Hue L, Viollet B, Guigas B. Metformin activates AMP-activated protein kinase in primary human hepatocytes by decreasing cellular energy status. *Diabetologia*. 2011 Dec;54(12):3101-10.
86. Miller RA, Chu Q, Xie J, Foretz M, Viollet B, Birnbaum MJ. Biguanides suppress hepatic glucagon signalling by decreasing production of cyclic AMP. *Nature*. 2013 Feb;494(7436):256-60.
87. Patel S, Srivastava S, Singh MR, Singh D. Preparation and optimization of chitosan-gelatin films for sustained delivery of lupeol for wound healing. *International journal of biological macromolecules*. 2018 Feb 1;107:1888-97.



88. Sahoo S, Chakraborti CK, Mishra SC, Naik S, Nanda UN. FTIR and raman spectroscopy as a tool for analyzing sustained release hydrogel of ciprofloxacin/carbopol polymer.
89. Vaingankar P, Amin P. Continuous melt granulation to develop high drug loaded sustained release tablet of Metformin HCl. *asian journal of pharmaceutical sciences*. 2017 Jan 1;12(1):37-50.
90. Razmjoo F, Sadeghi E, Rouhi M, Mohammadi R, Noroozi R, Safajoo S. Polyvinyl alcohol-Zedo gum edible film: Physical, mechanical and thermal properties. *Journal of Applied Polymer Science*. 2021 Feb 20;138(8):49875.
91. Hwang MR, Kim JO, Lee JH, Kim YI, Kim JH, Chang SW, Jin SG, Kim J, Lyoo WS, Han SS, Ku SK. Gentamicin-loaded wound dressing with polyvinyl alcohol/dextran hydrogel: gel characterization and in vivo healing evaluation. *Aaps Pharmscitech*. 2010 Sep;11(3):1092-103.
92. Hasatsri S, Pitiratanaworanat A, Swangwit S, Boochakul C, Tragoonsupachai C. Comparison of the morphological and physical properties of different absorbent wound dressings. *Dermatology research and practice*. 2018 May 21;2018.
93. Sanjoy K, Swagata DR, Bhusan SH. Development & optimization of pectin microsphere of metformin HCL. *International Journal of Drug Development and Research*. 2013;5(1):0-.
94. Ramhormozi P, Ansari JM, Simorgh S, Asgari HR, Najafi M, Barati M, Babakhani A, Nobakht M. Simvastatin accelerates the healing process of burn wound in Wistar rats through Akt/mTOR signaling pathway. *Annals of Anatomy-Anatomischer Anzeiger*. 2021 Jul 1;236:151652.
95. Venter NG, Monte-Alto-Costa A, Marques RG. A new model for the standardization of experimental burn wounds. *Burns*. 2015 May 1;41(3):542-7.
96. Wallace HA, Basehore BM, Zito PM. Wound healing phases.
97. Ali L, Ahmad M, Aamir MN, Minhas MU, Shah HH, Shah MA. Cross-linked pH-sensitive pectin and acrylic acid based hydrogels for controlled delivery of metformin. *Pakistan Journal of Pharmaceutical Sciences*. 2020 Jul 1;33(4).

98. Chinnaiyan SK, Karthikeyan D, Gadela VR. Development and characterization of metformin loaded pectin nanoparticles for T2 diabetes mellitus. *Pharmaceutical nanotechnology*. 2018 Dec 1;6(4):253-63.
99. Safdar B, Pang Z, Liu X, Jatoi MA, Mehmood A, Rashid MT, Ali N, Naveed M. Flaxseed gum: Extraction, bioactive composition, structural characterization, and its potential antioxidant activity. *Journal of food biochemistry*. 2019 Nov;43(11):e13014.
100. Jagdale SC, Patil SA, Kuchekar BS, Chabukswar AR. Preparation and characterization of Metformin hydrochloride– Compritol 888 ATO solid dispersion. *Journal of Young Pharmacists*. 2011 Jul 1;3(3):197-204.
101. Hafeez AE, Sara I, Eleraky NE, Hafez E, Abouelmagd SA. Design and optimization of metformin hydrophobic ion pairs for efficient encapsulation in polymeric drug carriers. *Scientific reports*. 2022 Apr 6;12(1):1-4.
102. Minoura N, Tsukada M, Nagura M. Physico-chemical properties of silk fibroin membrane as a biomaterial. *Biomaterials*. 1990 Aug 1;11(6):430-4.
103. Akhgari A, Farahmand F, Garekani HA, Sadeghi FA, Vandamme T. The effect of pectin on swelling and permeability characteristics of free films containing Eudragit RL and/or RS as a coating formulation aimed for colonic drug delivery. *Daru: Journal of Faculty of Pharmacy, Tehran University of Medical Sciences*. 2010;18(2):91.
104. Abuchowski A, Van Es T, Palczuk NC, Davis FF. Alteration of immunological properties of bovine serum albumin by covalent attachment of polyethylene glycol. *Journal of Biological Chemistry*. 1977 Jun 10;252(11):3578-81.
105. Xia C, Liang S, He Z, Zhu X, Chen R, Chen J. Metformin, a first-line drug for type 2 diabetes mellitus, disrupts the MALAT1/miR-142-3p sponge to decrease invasion

and migration in cervical cancer cells. *European Journal of Pharmacology*. 2018 Jul 5;830:59-67.

106. Zhao P, Sui BD, Liu N, Lv YJ, Zheng CX, Lu YB, Huang WT, Zhou CH, Chen J, Pang DL, Fei DD. Anti-aging pharmacology in cutaneous wound healing: effects of metformin, resveratrol, and rapamycin by local application. *Aging cell*. 2017 Oct;16(5):1083-93.
107. Schuiveling M, Vazirpanah N, Radstake TR, Zimmermann M, Broen JC. Metformin, a new era for an old drug in the treatment of immune mediated disease?. *Current drug targets*. 2018 Jun 1;19(8):945-59.
108. El-Bahy AA, Aboulmagd YM, Zaki M. Diabetex: A novel approach for diabetic wound healing. *Life sciences*. 2018 Aug 15;207:332-9.
109. Wynn TA, Vannella KM. Macrophages in tissue repair, regeneration, and fibrosis. *Immunity*. 2016 Mar 15;44(3):450-62.
110. Snyder RJ, Lantis J, Kirsner RS, Shah V, Molyneaux M, Carter MJ. Macrophages: a review of their role in wound healing and their therapeutic use. *Wound Repair and Regeneration*. 2016 Jul;24(4):613-29.
111. Sica A, Erreni M, Allavena P, Porta C. Macrophage polarization in pathology. *Cellular and molecular life sciences*. 2015 Nov;72(21):4111-26.
112. Leal EC, Carvalho E, Tellechea A, Kafanas A, Tecilazich F, Kearney C, Kuchibhotla S, Auster ME, Kokkotou E, Mooney DJ, LoGerfo FW. Substance P promotes wound healing in diabetes by modulating inflammation and macrophage phenotype. *The American journal of pathology*. 2015 Jun 1;185(6):1638-48.

113. Okizaki SI, Ito Y, Hosono K, Oba K, Ohkubo H, Amano H, Shichiri M, Majima M. Suppressed recruitment of alternatively activated macrophages reduces TGF- $\beta$ 1 and impairs wound healing in streptozotocin-induced diabetic mice. *Biomedicine & Pharmacotherapy*. 2015 Mar 1;70:317-25.
114. Yuan R, Geng S, Chen K, Diao N, Chu HW, Li L. Low-grade inflammatory polarization of monocytes impairs wound healing. *The Journal of pathology*. 2016 Mar;238(4):571-83.
115. Mirza RE, Fang MM, Novak ML, Urao N, Sui A, Ennis WJ, Koh TJ. Macrophage PPAR $\gamma$  and impaired wound healing in type 2 diabetes. *The Journal of pathology*. 2015 Aug;236(4):433-44.
116. Artlett CM. Inflammasomes in wound healing and fibrosis. *The Journal of pathology*. 2013 Jan;229(2):157-67.
117. Bitto A, Altavilla D, Pizzino G, Irrera N, Pallio G, Colonna MR, Squadrito F. Inhibition of inflammasome activation improves the impaired pattern of healing in genetically diabetic mice. *British journal of pharmacology*. 2014 May;171(9):2300-7.
118. Mirza RE, Fang MM, Weinheimer-Haus EM, Ennis WJ, Koh TJ. Sustained inflammasome activity in macrophages impairs wound healing in type 2 diabetic humans and mice. *Diabetes*. 2014 Mar 1;63(3):1103-14.
119. Pan Y, Sun X, Jiang L, Hu L, Kong H, Han Y, Qian C, Song C, Qian Y, Liu W. Metformin reduces morphine tolerance by inhibiting microglial-mediated neuroinflammation. *Journal of neuroinflammation*. 2016 Dec;13(1):1-2.
120. Jing Y, Wu F, Li D, Yang L, Li Q, Li R. Metformin improves obesity-associated inflammation by altering macrophages polarization. *Molecular and cellular endocrinology*. 2018 Feb 5;461:256-64.

121. Cosin-Roger J, Simmen S, Melhem H, Atrott K, Frey-Wagner I, Hausmann M, de Vallière C, Spalinger MR, Spielmann P, Wenger RH, Zeitz J. Hypoxia ameliorates intestinal inflammation through NLRP3/mTOR downregulation and autophagy activation. *Nature communications*. 2017 Jul 24;8(1):1-3.
122. Mehraj S, Sistla YS. Optimization of process conditions for the development of pectin and glycerol based edible films: Statistical design of experiments. *Electronic Journal of Biotechnology*. 2022 Jan 1;55:27-39.
123. D'Souza S. A review of in vitro drug release test methods for nano-sized dosage forms. *Advances in Pharmaceutics*. 2014 Nov 20;2014.
124. Li J, Chen J, Kirsner R. Pathophysiology of acute wound healing. *Clinics in dermatology*. 2007 Jan 1;25(1):9-18.
125. Abdel-Sayed P, Michetti M, Scaletta C, Flahaut M, Hirt-Burri N, de Buys Roessingh A, Raffoul W, Applegate LA. Cell therapies for skin regeneration: an overview of 40 years of experience in burn units. *Swiss medical weekly*. 2019 May 19;149(1920).